



UNIVERSITY OF VERONA

Department of Public Health and Community Medicine

GRADUATE SCHOOL

in

TRANSLATIONAL BIOMEDICINE

Director: Prof. Guido Francesco Fumagalli

DOCTORAL PROGRAM

in

FORENSIC MEDICINE AND SCIENCE

Coordinator: Prof. Franco Tagliaro

Series XXIV – Year 2009

With the financial support

of the

University of Padova

RADIOLOGICAL DETECTION

of

GUNSHOT RESIDUE

in

FIREARM WOUNDS

SSD MED/43 – Legal Medicine

Coordinator: *Prof. Franco Tagliaro*

Tutor: *Prof. Santo Davide Ferrara*

Ph.D. Student: *Dr. Giovanni Cecchetto*

To my father Attilio

CONTENTS

ABSTRACT	- 1 -
ABBREVIATIONS	- 3 -
INTRODUCTION	- 5 -
AIM OF THE RESEARCH PROJECT	- 7 -
REVIEW OF THE LITERATURE	- 9 -
GUNSHOT RESIDUE	- 9 -
THE FORMATION OF INORGANIC GSR PARTICLES	- 11 -
INORGANIC GSR ANALYSIS	- 12 -
<i>Color / Spot Testing</i>	- 12 -
<i>Neutron Activation Analysis</i>	- 12 -
<i>Atomic Absorption Spectrometry</i>	- 13 -
<i>Inductively Coupled Plasma</i>	- 14 -
<i>Scanning Electron Microscopy</i>	- 15 -
<i>Radiology</i>	- 16 -
MATERIALS AND METHODS	- 17 -
TARGETS	- 17 -
<i>Inclusion criteria</i>	- 17 -
<i>Exclusion criteria</i>	- 17 -
<i>Conservation process</i>	- 17 -
WOUNDS	- 18 -
<i>Gunshot wounds</i>	- 18 -
<i>Controls</i>	- 19 -
SAMPLES COLLECTION	- 20 -
<i>Fresh wounds</i>	- 20 -
<i>Decomposed wounds</i>	- 20 -
<i>Charred wounds</i>	- 22 -
VISUAL INSPECTION	- 22 -
MICRO-CT ANALYSIS	- 23 -
HISTOLOGICAL ANALYSIS	- 25 -
STATISTICAL ANALYSIS	- 26 -
<i>Fresh gunshot wounds</i>	- 26 -
<i>Decomposed and charred gunshot wounds</i>	- 26 -

RESULTS	- 27 -
FRESH GUNSHOT WOUNDS	- 27 -
<i>Macroscopic feature</i>	- 27 -
<i>Micro-CT feature</i>	- 27 -
<i>Histological feature</i>	- 27 -
<i>GSR amount</i>	- 30 -
DECOMPOSED GUNSHOT WOUNDS	- 35 -
<i>Macroscopic feature</i>	- 35 -
<i>Micro-CT feature</i>	- 35 -
<i>Histological feature</i>	- 35 -
<i>GSR amount</i>	- 38 -
CHARRED GUNSHOT WOUNDS	- 40 -
<i>Macroscopic feature</i>	- 40 -
<i>Micro-CT feature</i>	- 40 -
<i>Histological feature</i>	- 40 -
<i>GSR amount</i>	- 43 -
DISCUSSION	- 45 -
EXPERIMENTAL PROTOCOL	- 45 -
FRESH GUNSHOT WOUNDS	- 47 -
DECOMPOSED GUNSHOT WOUNDS	- 50 -
CHARRED GUNSHOT WOUNDS	- 54 -
LIMITS OF THE RESEARCH	- 58 -
CONCLUSIONS	- 59 -
REFERENCES	- 61 -
LIST OF ARTICLES, ABSTRACTS AND PRIZES	- 69 -
ACKNOWLEDGEMENTS	- 71 -

ABSTRACT

Introduction

Estimation of the firing range is often critical for reconstructing gunshot fatalities, where the main measurable evidence is the gunshot residue (GSR). After-death events, such as putrefaction, autolysis, incineration or extensive burning of the body, can alter the typical macroscopic and microscopic characteristics of firearm wounds, hampering or at least complicating the reconstruction of gunshot fatalities.

Aim of the research project

The present study aimed at evaluating and comparing the amount and differential distribution of GSR on fresh, decomposed, and charred gunshot wounds, utilizing a micro-computed tomography (micro-CT) analysis.

Materials and methods

A total of 110 experimental shootings at different firing distances (5, 15, 23, 30, and 40 cm) were performed on human calves surgically amputated for medical reasons. As controls we used 30 stab wounds, produced with an ice pick on calf sections.

Sixty specimens (10 for each tested distance and 10 stab wounds) were immediately formalin-fixed. Forty specimens (10 gunshot wounds from 5, 15, and 30 cm, and 10 stab wounds) were enclosed in a cowshed for 15 days, before formalin-fixation. Forty specimens (10 gunshot wounds from 5, 15, and 30 cm, and 10 stab wounds) were placed inside a wood-burning stove for 4 minutes at a temperature of 400°C.

All the samples were analysed by a micro-CT coupled to an imaging analysis software.

Results

Micro-CT analysis with three-dimensional image reconstruction detected GSR particles in all the investigated entrance wounds.

In fresh specimens, GSR was concentrated on the skin surface around the entrance hole, and in the epidermis and dermis layers around the cavity. In

decomposed specimens the high-density particles were detected only in the dermis layer. Regarding the charred wounds, the GSR deposits of the firearm lesions inflicted at very close distance (5 cm) were mainly constituted of huge particles with an irregular shape and well-delineated edges; at greater distances, agglomerates of tiny radiopaque particles scattered in the epidermis and dermis layers were evident. No GSR was detected in exit holes and stab wounds.

Statistical analysis showed a nonlinear relationship between the amount of GSR deposits and the firing range.

Conclusions

Our study, which is the first application of micro-CT analysis in the field of forensic ballistics, demonstrates that micro-CT could be an objective and rapid tool for the analysis of gunshot wounds in firearm fatalities. On fresh samples, this method may be of practical use for estimating the firing range given a known percentage of the GSR deposit, while in bodies in advanced decomposition or extremely damaged by fire, it might furnish precious information on the nature and means of productions of an injury, playing an important role for reconstructing the shooting incident.

For estimating the sensitivity and specificity of the proposed method, it will be necessary to test the micro-CT, analysing specimens of forensic caseworks and confirming the positive results with a “*gold-standard*” method.

ABBREVIATIONS

AES: atomic emissions spectroscopy

AAS: atomic absorption spectrometry

Avg: average

B: bullet

Ba: barium

BC: bullet core

BJ: bullet jacket

BP: black powder

C: case

CDR: cartridge discharge residue

CI: confidence interval

EDX: X-rat detector energy dispersion

ESEM: Environmental scanning electron microscope

FOV: field of view

GSR: gunshot residue

HU: Hounsfield units

ICP: inductively coupled plasma

LFPM: lead free primer mix

Max: maximum

Micro-CT: micro-computed tomography

Min: minimum

MS: mass spectrometry

NAA: neutron activation analysis

P: primer

Pb: lead

PC: primer cup

PM: primer mix

PP: propellant powder

Abbreviations

RH: relative humidity

RIB: rust inside barrel

Sb: antimony

SD: standard deviation

SEM: scanning electron microscope

VOI: volume of interest

INTRODUCTION

Ballistics is the science of bodies in flight, encompassing the physical phenomena involved and the movement of the projectile. It is divided into a number of areas, based on where the projectile is: interior ballistics, external ballistics, and terminal ballistics [Kneubuehl BP et al, 2011].

Interior ballistics is the study of the acceleration of the bullet in the weapon and the related processes. The domain of interior ballistics ends where the bullet leaves the barrel [Kneubuehl BP et al, 2011].

Exterior ballistics is the study of the projectile through air [Di Maio VJM, 1999]. This part of ballistics involves determining the changes over time and space of the trajectory of the bullet, its velocity and the movements it describes about its centre of gravity, taking into account all the forces acting upon it.

The study of the phenomena occurring when a bullet strikes and penetrates an object is termed *terminal ballistics* [Kneubuehl BP et al, 2011].

Wound ballistics can be considered a subdivision of terminal ballistics concerned with the motions and effects of the projectile in animal or human tissue. The location, size, and the shape of the temporary cavity in a body depend on the amount of kinetic energy lost by the bullet in its path through the tissue, how rapidly the energy is lost, and the elasticity and cohesiveness of the tissue. The structure of the bullet and certain aspects of the weapon may also play a role [Di Maio VJM, 1999].

Forensic ballistic can be briefly defined as the application of ballistics for forensic purposes. Forensic medicine uses the laws of wound ballistics to derive ballistic data (type of weapon and ammunition, direction of shot, range, etc.) required to elucidate killings involving firearms. The major task of this discipline is the reconstruction of the events that produced a gunshot injury, fatal or not (Karger, 2008).

Even if the very basis is formed by wound ballistics, a large variety of additional findings and evidence can be utilized for reconstructing the events leading to a gunshot injury, such as gunshot residue (GSR) or the geometry of the bullet tract.

AIM OF THE RESEARCH PROJECT

The evaluation of the firing range has often a critical importance in gunshot fatalities [Sellier K, 1991]. When the issue of suicide, homicide and accidental firing is in question, the investigation of GSR particles gains extensive forensic significance [Nag NK et al, 1992].

These products of firearm discharge are principally composed of burnt and unburnt particles from the propellant, as well as components from the primer, the bullet and its jacket, and from the cartridge case [Matty W, 1982]. The amount and distribution of GSR reaching the target surface, are generally considered to be related to the firing range [Brown H et al, 1999]. In the past, forensic scientists have studied the distribution of GSR at the entrance wound using a variety of methods.

Recently micro-computed tomography (micro-CT), a tomographic technique with a spatial resolution of a few microns, has opened the possibility of performing tri-dimensional histological investigations on a virtual representation of the sample [Cnudde V et al, 2008].

The present research aimed at testing this novel application for the evaluation and determination of GSR in gunshot wounds.

The specific aims were as follows.

1. To elaborate a standardized experimental protocol, using human skin samples and fixed stands, in order to produce fresh intermediate-range gunshot-wounds, as well as decomposed and charred firearm injuries.
2. To analyze the samples by means of a Micro-CT coupled to an imaging analysis software.
3. To generate 3D-reconstruction of the entry and exit wounds in order to identify the spatial distribution of GSR deposit in the soft tissue around the cavity.
4. To quantify the amount of GSR, calculated as the proportion of the volume of interest (VOI) occupied by metal particles.

5. To verify if the percentage of inorganic residues in fresh gunshot wounds correlates to the shooting distance.
6. To determine the effect of after-death events, such as putrefaction/autolysis changes or fire effect, on the distribution of GSR in the skin specimens.

REVIEW OF THE LITERATURE

Gunshot Residue

Gunshot residue, which may also be known as cartridge discharge residue (CDR) or firearms discharge residue are particles produced during the discharge of a firearm. When a cartridge/round is fired in a firearm, combustion products from both the primer and the propellant will be released at the same time [Warlow TA, 1996].

Gunshot residues are composed of unburned and partially burnt propellant powder, particles from the ammunition primer, smoke, grease, lubricants, and metals from the cartridge as well as the weapon itself [Morales EB et al, 2004; Romolo FS et al, 2001).

Organic compounds mainly originate from propellant and firearm lubricants, taking the form of unburned and partially burned gunpowder particles, some products of their transformation, and hydrocarbons (table n. 1).

Inorganic residues such as nitrates, nitrites, and metallic particles originate from the primer and propellant as well as the cartridge case, the projectile jacket or its core and from the weapon barrel itself [Brozek-Mucha Z et al, 2001] (table n. 1).

These combustion materials from the primer, propellant, and other sources escape from weapon openings and vaporized materials solidify into particulates. These particulates are usually of sizes ranging from 0.5 μm to 10 μm (diameter), although sizes of up to 100 μm have been reported [Schwoeble AJ et al, 2000].

Table 1. Compounds that may contribute to gunshot residue

Organic		Inorganic	
Compound	Source of Compound	Compound	Source of Compound
2,4,6-Trinitrotoluene (TNT)	PPPM	Aluminum	PC
2,4-Dinitrodiphenylamine (2,4-DPA)	PP	Aluminum sulfide	PM
2,3-Dinitrotoluene (2,3-DNT)	PP	Antimony	C/B
2,4-Dinitrotoluene (2,4-DNT)	PP	Antimony sulfide	PM
2,6-Dinitrotoluene (2,6-DNT)	PP	Antimony sulfite	PM
2-Nitrodiphenylamine (2-NDPA)	PP	Antimony trisulfide	PM
4-Nitrodiphenylamine (4-NDPA)	PP	Arsenic	C
Akaridte II (AKII)	PP	Barium nitrate	PM/PP
Butyl phthalate	PP	Barium peroxide	PM
Butylcentralite (N,N-Dibutylcarbanilide)	PP	Bismuth	C
Camphor	PP	Boron	PM
Carbanilide	PP	Brass	C
Carbazole	PP	Bronze	B
Charcoal (major carbon)	BP	Calcium carbonate	PP
Cresol	PP	Calcium silicide	PM
Dextrin	PM	Chromium	B
Diazodinitrophenol	PM	Copper	BJ/PC/C
Diazonitrophenol	PM	Copper thiocyanate	PM
Dibutyl phthalate	PP	Cupro-nickel	BJ
Diethyl phthalate	PP	Gold	PM
Dimethyl phthalate	PP	Ground glass	PM
Dimethylsebacate	PP	Iron	RIB/B
Dinitrocresol	PP	Lead	B
Diphenylamine (DPA)	PP	Lead azide	PM
Ethyl centralite (N,N-Diethylcarbanilide)	PP	Lead dioxide	PM
Ethyl phthalate	PP	Lead nitrate	PM
Ethylene glycol dinitrate	PP	Lead peroxide	PM
Gum Arabic	PM	Lead stiftate (styphnate)	PM
Gum tragacanth	PM	Lead thiocyanate	PM
Karaya gum	PM	Magnesium	PM
Methyl cellulose	PP	Mercury	PM
Methyl centralite(N,N-Dimethylcarbanilide)	PP	Mercury fulminate	PM
Methyl phthalate	PP	Nickel	C
Nitrocellulose (NC)	PP/PM	Nitrate	BP
Nitroglycerine (NG)	PP/PM	Phosphorus	C
Nitroguanidine	PP	Potassium chlorate	PM
Nitrotoluene	PP	Potassium nitrate	PP/PM
N-nitrosodiphenylamine (N-NDPA)	PP	Prussian blue	PM
Pentaerythritol tetranitrate (PETN)	PP/PM	Red brass	BJ
Picric acid	PP	Silicon	PM
RDX (Cyclonite)	PP	Sodium nitrate	PM
Resorcinol	PP	Sodium sulphate	PP
Rubber cement	PM	Steel	BCC
Sodium Alginate	PM	Strontium nitrate	PM
Starch	PP	Sulphur	PM/BP
Tetracene	PP/PM	Tin	PM
Tetryl	PP/PM	Titanium	PMLFPM
Triacetin	PP	Tungsten	B
		Yellow brass	BJC
		Zinc	PC
		Zinc peroxide	PM
		Zirconium	PM

B: bullet - **BC:** bullet core - **BJ:** bullet jacket - **BP:** black powder - **C:** case
LFPM: lead free primer mix - **P:** primer - **PC:** primer cup - **PM:** primer mix
PP: propellant powder - **RIB:** rust inside barrel

The Formation of Inorganic GSR Particles

Gunshot residue particles form during the discharge of a firearm. As the firing pin strikes the primer cap, the primer mixture is ignited, creating an environment of rapid temperature and pressure increases within the cartridge. This increase in temperature melts the primer mixture and within a few milliseconds the vaporization points of lead (Pb), barium (Ba), and antimony (Sb) are exceeded (Pb 1620/C, Ba 1140/C, Sb 1380/C). The effects of supersaturation cause vaporized particles to condense back onto the liquefied primer surface as droplets.

There has been evidence to suggest that inorganic GSR particles of materials originating solely from the primer (primer GSR) are formed even before the propellant is ignited [Basu S, 1982].

As the primer mix ignites the propellant powder, a second rapid increase in pressure and temperature occurs and the bullet is expelled from the firearm barrel. During this process, the particles involved are subjected to extreme temperature and pressure followed by rapid cooling. Particles form as liquid droplets, which subsequently solidify [Basu S, 1982].

Wolten and Nesbitt suggested that GSR particles formed from inorganic substances can be divided into two categories, “*primer particles*” and “*bullet particles*”.

Primer particles were shown to contain oxides, sulfides and salts in which the anion contained oxygen (oxysalts), such as barium meta-antimonate and basic lead sulfate (lanarkite). It was reported that primer ingredients are initially compounds and therefore cannot be expected to be reduced to elements in the oxidizing environment of the primer ignition. Elemental particles should therefore originate from bullet materials (Wolten GM et al, 1979).

Inorganic GSR Analysis

Color/Spot Testing

Color/spot tests are most commonly used for the estimation of firing distances [Schwoeble AJ et al, 2000]. However, they can also be used as a rapid test for the presence of GSR and the determination of bullet holes/entrance wounds.

Such tests have been in use since 1933, when the dermal nitrate or paraffin test was introduced [Romolo FS et al, 2001; Meng HH et al, 1997].

The main problem that arises from using spot / color tests is their presumptive nature. However, despite this, histochemical techniques, such as Alizarin Red S [Tschirhart DL et al, 1991; Brown H et al, 1999] or sodium rhodizonate [Marty W et al, 2002; Neri M et al, 2007; Tugcu H et al, 2006; Andreola S et al, 2011] are still used in forensic case works for determining the presence of GSR.

Neutron Activation Analysis

Neutron activation analysis (NAA) has been used as a bulk analysis method for various elements, which can be found in inorganic GSR. Ba and Sb are the two main elements identified using this method (Rudzitis E et al, 1973; Rudzitis E et al, 1975; Ruch RR et al, 1964; Krishnan SS, 1967).

Capannesi and Sedda used NAA to examine the trace elements present in lead core, jacketed bullet fragments [Capannesi et al, 1992]. NAA has also been used for the determination of firing distances [Krishnan SS, 1974] and the determination of GSR on the hands of shooters [Rudzitis E et al, 1975; Krishnan SS, 1974; Pillay KKS et al, 1974].

A number of problems have been reported with NAA; the technique cannot be applied to Pb analysis, samples must be irradiated, which requires a nuclear reactor as a neutron source, trained personnel are required to carry out the analysis procedure [Romolo FS et al, 2001], and it is also an expensive and time consuming technique [Schwoeble AJ et al, 2000].

Atomic Absorption Spectrometry

Conventional atomic absorption spectrometry (AAS) has been reported sensitive enough for the detection of Pb in GSR samples, but inadequate for Ba and Sb. However, the introduction of electro thermal atomizers (carbon rod, tantalum, and graphite tube furnace) made flameless AAS suitable for the analysis of Ba and Sb in GSR samples [Romolo FS et al, 2001]. Samples are most commonly collected using cotton-tipped swabs and 5% nitric acid [Cooper R et al, 1994; Koons RD et al, 1987].

Flameless AAS has been reported as a successful technique for the analysis of inorganic GSR as it is both readily available and cost effective [Can M et al, 2003]. It has an advantage over NAA, having excellent sensitivity for Ba and Sb and can be used to detect other elements of interest including Pb [Koons RD, 1993].

AAS has been applied to the determination of shooting distances, based on concentration patterns of Pb around bullet holes, [Krishnan SS, 1974] and the detection of GSR on collection swabs taken from hands by the determination of antimony and barium concentrations [Koons RD, 1993].

Ravreby reported the use of flame and flameless AAS for the analysis of residues collected from bullet holes. Elements originating from the bullet, case, primer and firearms were analyzed. The results provided a means for identifying the type of ammunition used [Ravreby M, 1982].

Koons discussed a number of problems associated with AAS. Incomplete extraction of Sb from collection swabs was shown to be an issue; even with an optimized method only 60–70% was extracted, compared to a nearly complete extraction of Pb and Ba. Further problems arising from the extraction process included variable absorbance-time profiles for Sb and the enhancement of Ba absorbance caused by various matrix constituents [Koons RD et al, 1987].

The worth of AAS in term of GSR analysis was further brought into question by Aleksandar, who criticized the method on the basis of the large

number of false negative results it has been shown to produce (about 40%) [Aleksandar I, 2003].

Inductively Coupled Plasma

Inductively coupled plasma (ICP) is a bulk analysis technique that is usually used to analyze trace amounts of Pb, Ba, and Sb in primer residues [Schwoeble AJ et al, 2000].

Koons reported the use of ICP with atomic emissions spectroscopy (AES) for the analysis of Ba levels in swabs [Koons RD et al, 1988]. The method was determined more successful than the previously used AAS because of the lack of interference from common swab constituents, a wide linear dynamic range, and good precision and accuracy.

Koons also reported the use of ICP-MS for the analysis of residues originating from primers [Koons RD, 1998]. The use of MS allowed the detection of several isotopes for each of the elements of interest (Pb, Ba, Sb). ICP-MS was reported as potentially useful in several areas; the determination of levels of additional elements which may be associated with the handling of a firearm or ammunition component, or elements which may be present in specific ammunitions.

Steffen et al reported the use of ICP-MS in conjunction with SEM-EDX [Steffen S et al, 2007].

Sarkis employed sector field, high-resolution-ICP-MS to determine the levels of Pb, Ba, and Sb in residue samples, allowing identification of these elements at concentrations as low as 1 ng/mL. Ternary graphs were used to better visualize the results and allow direct comparisons between the relative percentages of the three compounds of interest in different samples. Such graphs were reported to provide strong evidence concerning the origins of sample components on hands (GSR or environmental) [Sarkis JES et al, 2007].

Scanning Electron Microscopy

Scanning electron microscope equipped with an X-ray detector (wavelength dispersion, or energy dispersion [EDX]) is the most commonly used method of analyzing inorganic GSR [Romolo FS et al, 2001].

The advantage that SEM and X-ray detection has over bulk analysis techniques is the ability to analyze individual particles of inorganic GSR both morphologically and chemically, making it possible to determine that particles could have only originated from the discharge of a firearm and no other way. Despite this SEM-EDX cannot determine whether a person discharged a weapon on any given occasion [Aleksandar I, 2003].

Lebiedzki and Johnson reported the use of specific morphological and elemental indicators within inorganic GSR particles to differentiate between the firearm used to discharge a round, the case and bullet material of the ammunition and ultimately differentiate one type of ammunition from another [Lebiedzki J et al, 2004].

One of the biggest drawbacks to SEM analysis was the tedious and time-consuming task of manual particle searching within samples.

The introduction of automated GSR search programs has eliminated such a problem, reducing the total search time for a sample, freeing the SEM operator to do other tasks and reducing the number of potential human error sources [White RS et al, 1987].

Germani investigated the effects of changing SEM-EDX variables on search results, in an attempt to compile a set of standard settings for the analysis of inorganic GSR particles. It was reported that no one set of standard operating procedures could be determined, as the required search parameters between different samples are likely to be variable [Germani MS, 1991].

Radiology

Radiographic techniques potentially offer quicker non-invasive analysis tools for the detection of GSR and could provide valuable information in the forensic assessment of patients with gunshot wounds.

Schyma described fine metallic residues which can be detected by microradiography after shooting pigskin [Schyma et al, 1996]. Pluisch and Sellier examined whether metal particles could be detected by radiology if vertebral bodies had been hit by unjacketed small calibre lead bullets. They were able to show that for all shots with such bullets so called “lead paths” were present along the intravertebral bullet track [Pluisch et al, 1994].

Stein et al distinguished very close-range shots from shots from a range of more than 5 cm using a routine CT. In contact shots, regular and reproducible radiopaque rings in the fatty tissue could be seen which showed a conical form penetrating into the depth. For unjacketed bullets, radiopaque material could be seen after firing ranges of up to 10 cm, for jacketed bullets the radiopaque material was completely missing in the wound after firing ranges of 5 cm and above [Stein KM et al, 2000].

Rutty et al analyzed gunshot wound by means of a modern 16 slice multi-detector CT scanner. Using anterior–posterior and lateral scout views and multiplane reconstructed images, it was possible to visualize the temporary cavity, as well as the fragmentation and dispersal pattern of the projectiles, the distance travelled and angle of dispersal within the block of each projectile or fragment [Rutty GN et al, 2008].

MATERIALS AND METHODS

Targets

After approval of the Ethical Committee of the University-Hospital of Padova (Protocol n. 2013P), 140 sections of approximately 6 cm in length were obtained from human calves using a saw (Fig. 1-2).

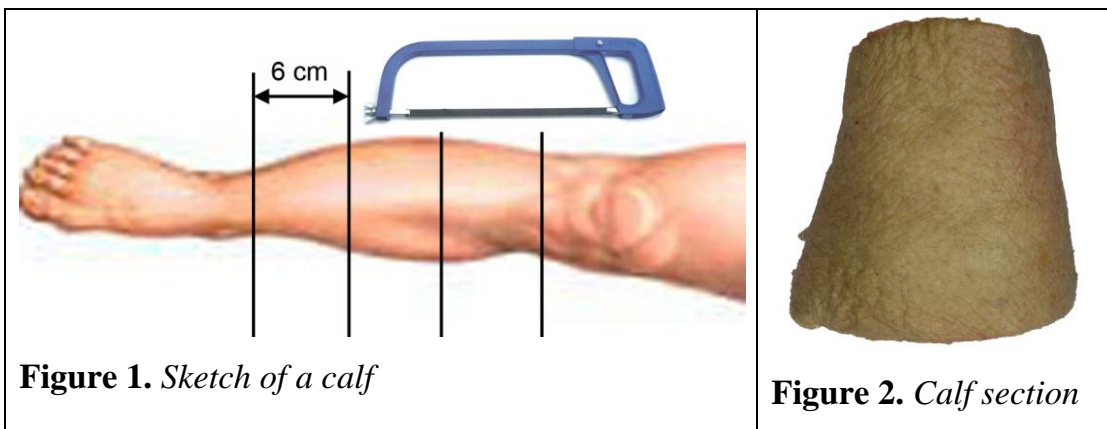
Each calf was been surgically amputated for medical reasons (circulatory disorders, road or workplace trauma).

Inclusion criteria

- Male sex.
- Age between 20 and 50 years.

Exclusion criteria

- Neoplastic and/or inflammatory and/or infective diseases of the skin.
- Scars.
- Traumatic skin wounds.



Conservation process

Three hours after the surgical amputation, each calf section was washed to remove dirt, dried blood and any other contaminants from the skin surface, and keep frozen at -20°C until the day before the shooting experiments, when all the samples were defrosted in open air for 12 hours.

Wounds

Gunshot wounds

To produce gunshot wounds, we carried out shooting experiments in a ballistic laboratory at distances of 5, 15, 23, 30, and 40 cm, using a 7.65 mm semi-automatic pistol (Beretta mod. 81 – Fig. 3) loaded with 7.65x17 mm Browning SR full metal jacketed bullets (Fig. 4).

All the ammunitions came from the same production lot.

The firearm was placed on a fixed stand and the surface of the skin sample was kept perpendicular to the muzzle of the gun (Fig. 5).

A total of 110 shots were performed as follows:

- 30 times at 5 cm;
- 30 times at 15 cm;
- 10 times at 23 cm;
- 30 times at 30 cm;
- 10 times at 40 cm.



Figure 3. *Beretta mod. 81*



Figure 4. *Browning SR full metal jacketed bullet*

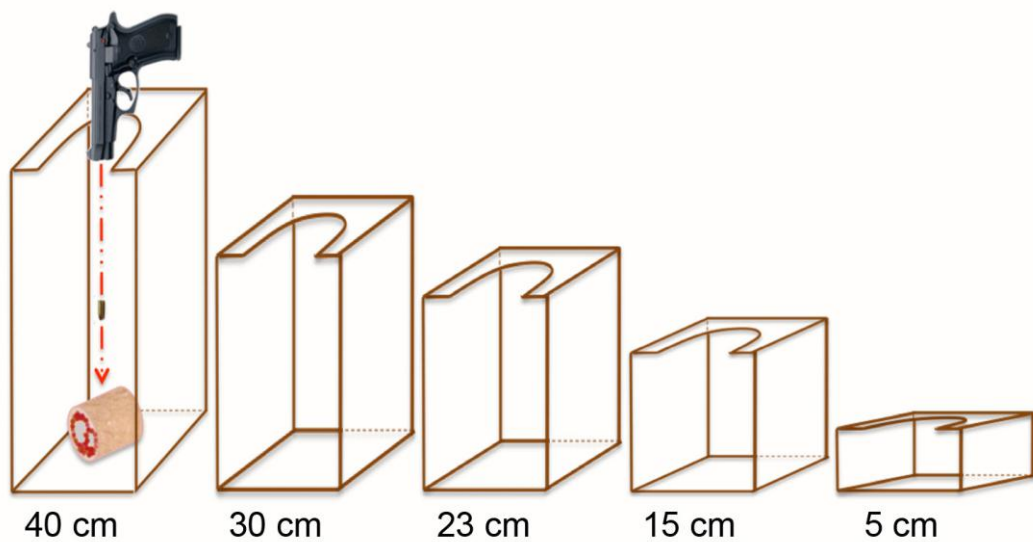


Figure 5. *Sketch of the stands used to perform the firing trials*

Controls

As controls we used 30 stab wounds, produced with an ice pick on calf sections.

Samples collection

In order to estimate the diagnostic efficiency of micro-CT analysis in normal conditions, as well as in extreme conditions often encountered in forensic practice, the leg sections have been processed as follows.

Fresh wounds

Sixty calf sections (10 gunshot wounds for each firing distance tested and 10 stab wounds) were immediately formalin fixed (4%, pH 7.4) for 3 days.

Decomposed wounds

Forty calf sections (10 gunshot wounds from 5 cm, 10 gunshot wounds from 15 cm, 10 gunshot wounds from 30 cm, and 10 stab wounds) were enclosed inside plastic boxes covered by mosquito nets to avoid the maggot infestation (Fig. 6), and placed in a cowshed for 15 days, before formalin fixation. The decomposing changes affecting the gunshot lesions were documented at 24 hours intervals. The ambient air temperature, recorded hourly, ranged from a high of 38°C to a low of 11°C (Fig. 7). The relative humidity ranged from a high of 100% to a low of 25% (Fig. 8).



Figure 6. *Plastic box and calf sections*

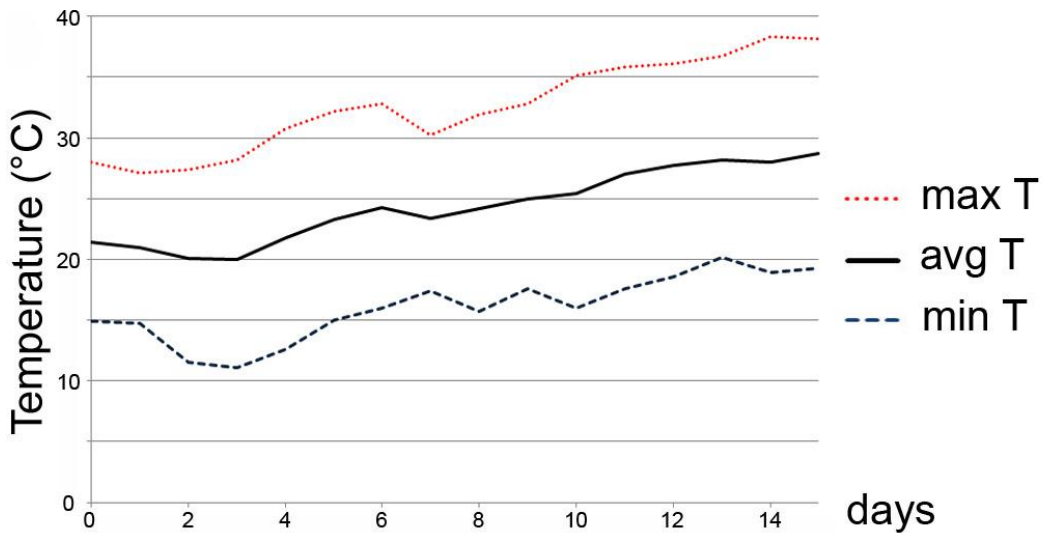


Figure 7. *Graphs showing the ambient air temperature during the experimental period*

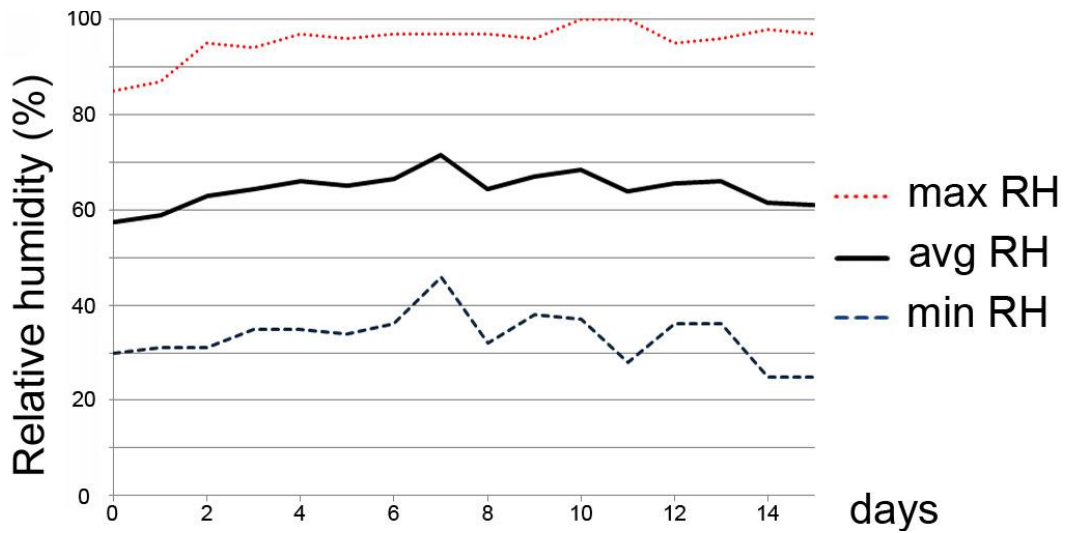


Figure 8. *Graphs showing the ambient relative humidity during the experimental period*

Charred wounds

Forty calf sections (10 gunshot wounds from 5 cm, 10 gunshot wounds from 15 cm, 10 gunshot wounds from 30 cm, and 10 stab wounds) were placed inside a wood-burning stove for 4 minutes at a temperature of 400°C (Fig. 9).



Figure 9. *Calf section inside the wood-burning stove*

Visual inspection

The macroscopic feature of the lesions was documented immediately after the firing tests using a digital camera (Nikon D-90 equipped with AF-S Nikkor 18-105 mm ED, Nikon Corporation, Shinjuku, Japan) (Fig. 10).



Figure 10. *Nikon D-90*

Micro-CT Analysis

Two specimens, comprising the epidermis, dermis and subcutaneous fat around the wounds were obtained from each calf section, cut into parallelepipeds (height 1 cm, side 1 cm) with the hole in the middle using a lancet (Fig. 11), and then located in a cylindrical polyethylene container (1.1-cm-diameter) with formalin (4%, pH 7.4) for 3 days.

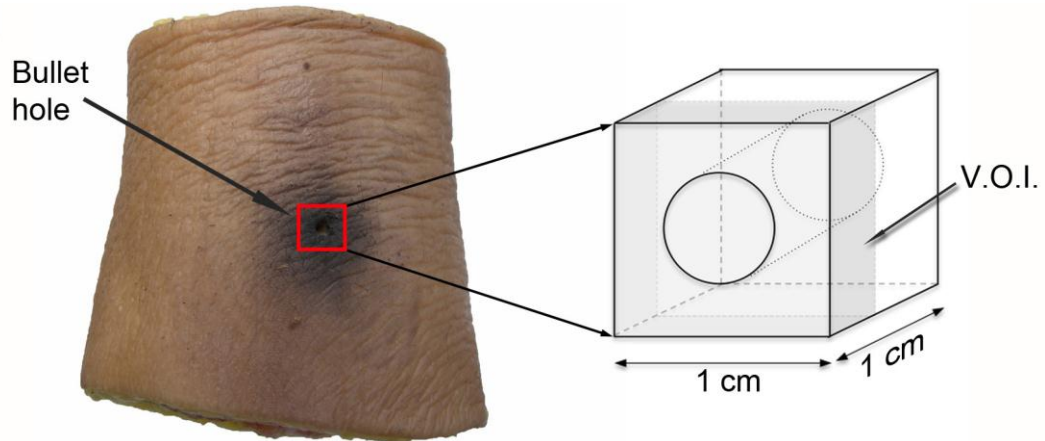


Figure 11. Diagram showing the preparation of a skin sample for micro-CT analysis; the VOI has a side of 1 cm and a height of 3,8 mm

All specimens were scanned using a Skyscan 1172 HR Micro-CT (Skyscan, Aartselaar, Belgium) (Fig. 12).

Micro-CT settings were as follows:

- 100kV of voltage;
- 100 μ A of current;
- filter of aluminium with 1 mm of thickness to reduce the beam hardening artefact;
- 1280 x 1024 pixel of Field of View (FOV);
- 13 μ m of isotropic voxel size.

All samples underwent a 360° rotation, with a rotation step of 0.4 degree and a frame averaging of 2. The acquired raw data were reconstructed with a N-Recon software (Skyscan, Aartselaar, Belgium) which uses the back-projection algorithm to reconstruct axial subsequent images saved as bitmap

format. To calibrate the Hounsfield Units (HU), one water phantom was acquired and reconstructed at the same sample settings.

The bitmap images were analyzed by a CT-An Software (Skyscan, Aartselaar, Belgium): the selected VOI (side of 1 cm and height of 3,8 mm) was focused into the center of the specimen in order to position the entire entry wound in the middle. All the samples were binarized using the same parameters. Since GSR deposits are mainly formed of heavy metal particles (such as barium, antimony, lead, etc.), their percentage (considered as the proportion of the VOI occupied by binarised solid objects) was calculated analyzing all particles with a density higher than 1000 HU (particles with a density lower than 1000 HU were excluded to reduce iron artefacts). The 3D images were reconstructed through a CT-Vox Software (Skyscan, Aartselaar, Belgium).



Figure 12. *Skyscan 1172 HR Micro-CT*

Histological analysis

Preparation of skin sections for light microscopy involved bisecting the wound site using a sharp scalpel. Each skin sample was embedded in paraffin block by routine overnight processing. Paraffin sections 5- μ m thick were cut from each block using a rotary microtome. Subsequently, each slide was deparaffinized, hydrated by distilled water, stained with hematoxylin-eosin, and examined with a Leica DM-4000B optical microscope (Leica, Cambridge, UK) (Fig. 13).



Figure 13. *Leica DM-4000B*

Statistical analysis

For each type of samples (fresh, decomposed, charred) and for each firing distance tested, the amount of GSR particles was expressed as means \pm standard deviations.

Fresh gunshot wounds

Statistical analysis comprised two main phases. In phase 1, through a curve fitting process, the mathematical model which best described the relationship between GSR percentages and the firing distances was chosen, and the R² index was calculated.

The statistical estimation of the model applied to our data was performed through a PROC NLIN procedure with the software SAS®9.2 (SAS Institute INC, Cary, North Carolina). Subsequently, the 95% Confidence Interval (95%CI) of the interpolation function was calculated.

In phase 2, the target was the estimation of the firing distance based on a given GSR percentage. Thus, a mathematical model derived from the inversion of the interpolation function was calculated. The parameters of the model were estimated using a PROC NLIN procedure with the software SAS®9.2 (SAS Institute INC, Cary, North Carolina). The 95%CI was calculated for a single firing distance.

Decomposed and charred gunshot wounds

Comparison between mean GSR values of fresh and altered samples was performed with two-way ANOVA test. Subsequent analysis of mean GSR percentages at the three tested firing distances (5 cm, 15 cm, and 30 cm) between groups (fresh vs decomposed samples and fresh vs charred samples) was conducted with the Bonferroni t-test.

RESULTS

Fresh gunshot wounds

Macroscopic feature

The fresh entrance lesions exhibited the typical characteristics of intermediate range gunshot wounds [Nag NK et al, 1992]; at close examination, individual powder particles embedded in the skin were always evident, and the intensity of the skin blackening decreased with the increase of the firing range as expected (Fig. 14).

The exit wounds were larger than entrance wounds, with everted margin, and did not present a bullet wipe, powder particles, and blackening.

Stab wounds presented a central skin defect with well-delineated edges, and a diameter similar to that of gunshot wounds.

Micro-CT feature

At micro-CT analysis, a clearly decreasing trend in the mean GSR area was observed by increasing the firing distance. In particular, the amount of GSR particles (density higher than 1000 HU) was noticeably reduced when the shot was fired from more than 30 cm, compared with firing ranges of less than 23 cm. For the 5, 15, and 23 cm distances, the GSR were concentrated on the skin around the hole, in the epidermis and dermis layers, and inside the cavity, while, at greater distances, they were deposited mainly on the skin surface. No GSR particles were detected in control specimens, neither in the exit holes (Fig. 14-15).

Histological feature

In entrance gunshot wounds, smoke stain and gunpowder interspersions were well evident on the surface of the epidermis.

No gunpowder interspersions were evident in exit holes and stab wounds (Fig. 14).

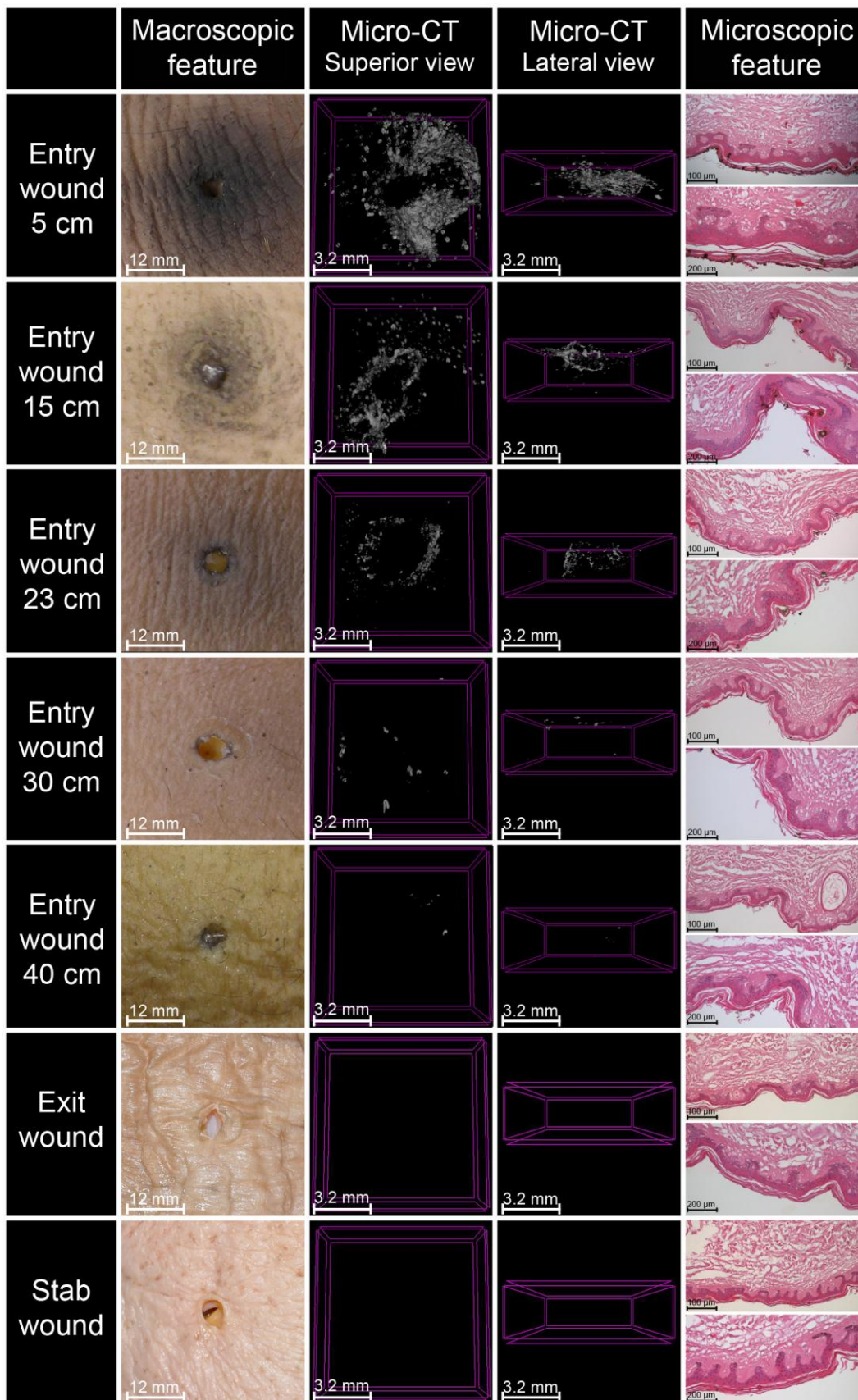


Figure 14. Macroscopic, radiological and microscopic features of fresh gunshot wounds

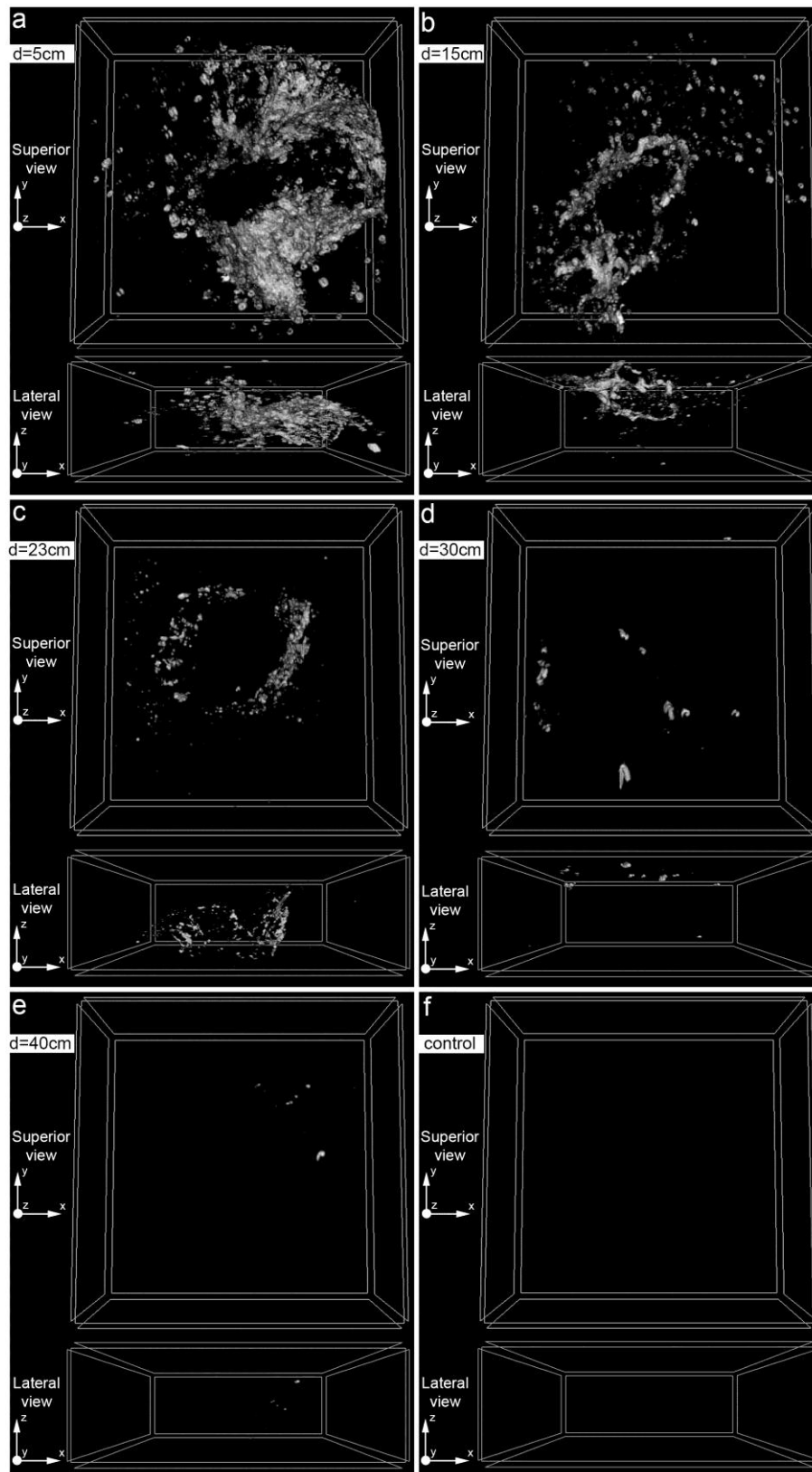


Figure 15. 3D reconstructions of fresh gunshot wounds at different firing distances. Only particles of density higher than 1000 HU are shown

GSR amount

The mean percentages of GSR deposits for each tested firing distance are listed in Table n. 2.

Statistical analysis showed a nonlinear relationship between the amount of GSR deposits and the firing range (Fig. 16). A negative exponential model ($R^2=0.9749$), and a 2nd order polynomial model ($R^2=0.9725$) were fit to the experimental data appearing, however, poorly performing. A Gaussian model was found to better describe the relationship between the firing distance (independent variable “x”) and the GSR percentage (dependent variable “y”) ($F[2;48]=1919.7$, $P<0.0001$; $R^2=0.9876$) (Fig. 17). The estimated function of the model is:

$$y = 0.4646 * \exp [- (x / 16.3134)^2]$$

The algebraic inversion of the above-reported function and the statistical evaluation of its parameters permitted to estimate the relationship between GSR percentages (independent variable “x”) and the firing distances (dependent variable “y”) ($F[2;48]=2609.03$, $P<0.0001$; $R^2=0.9909$) (Fig. 18):

$$y' = [-200.5803047 - 273,4318654 * \ln(x')]^{1/2}$$

The distance values and their 95%CI estimated on the basis of a number of GSR percentages are reported in Table n. 3.

Table 2. Results of the shooting trials.

Analysis Variable: GSR percentage					
Firing range	Shots number	Mean	SD	Minimum	Maximum
Entry wound 5 cm	10	0.420	0.038	0.370	0.470
Entry wound 15 cm	10	0.211	0.021	0.180	0.250
Entry wound 23 cm	10	0.044	0.011	0.030	0.060
Entry wound 30 cm	10	0.028	0.018	0.010	0.050
Entry wound 40 cm	10	0.002	0.001	0.001	0.003
Exit wound	10	0.000	0.000	0.000	0.000
Stab wound	10	0.000	0.000	0.000	0.000

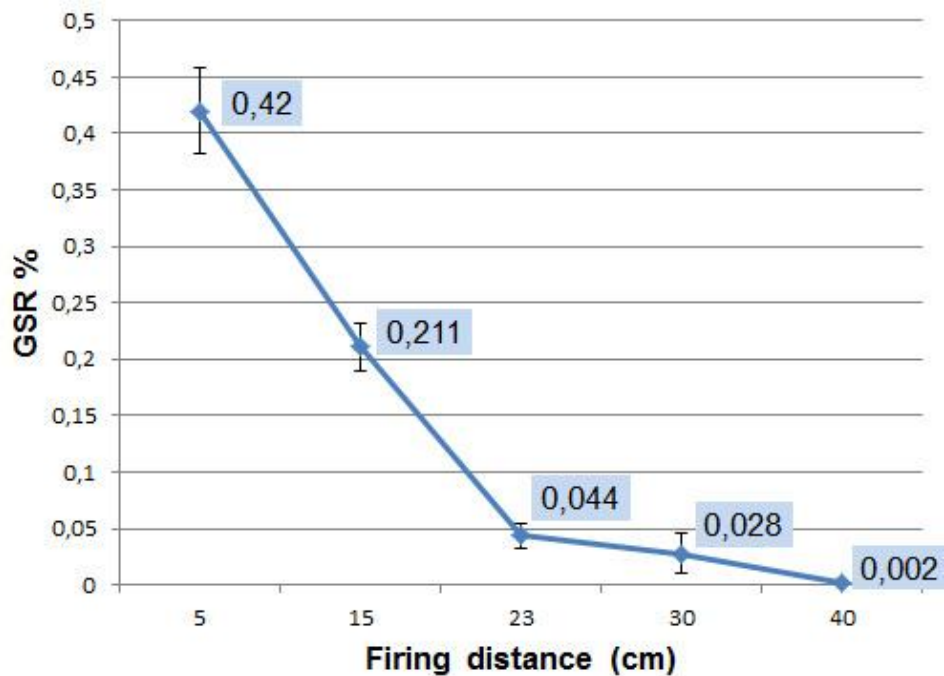


Figure 16. Graphs showing the GSR concentrations detected by micro-CT analysis in fresh gunshot wounds inflicted at different firing distances

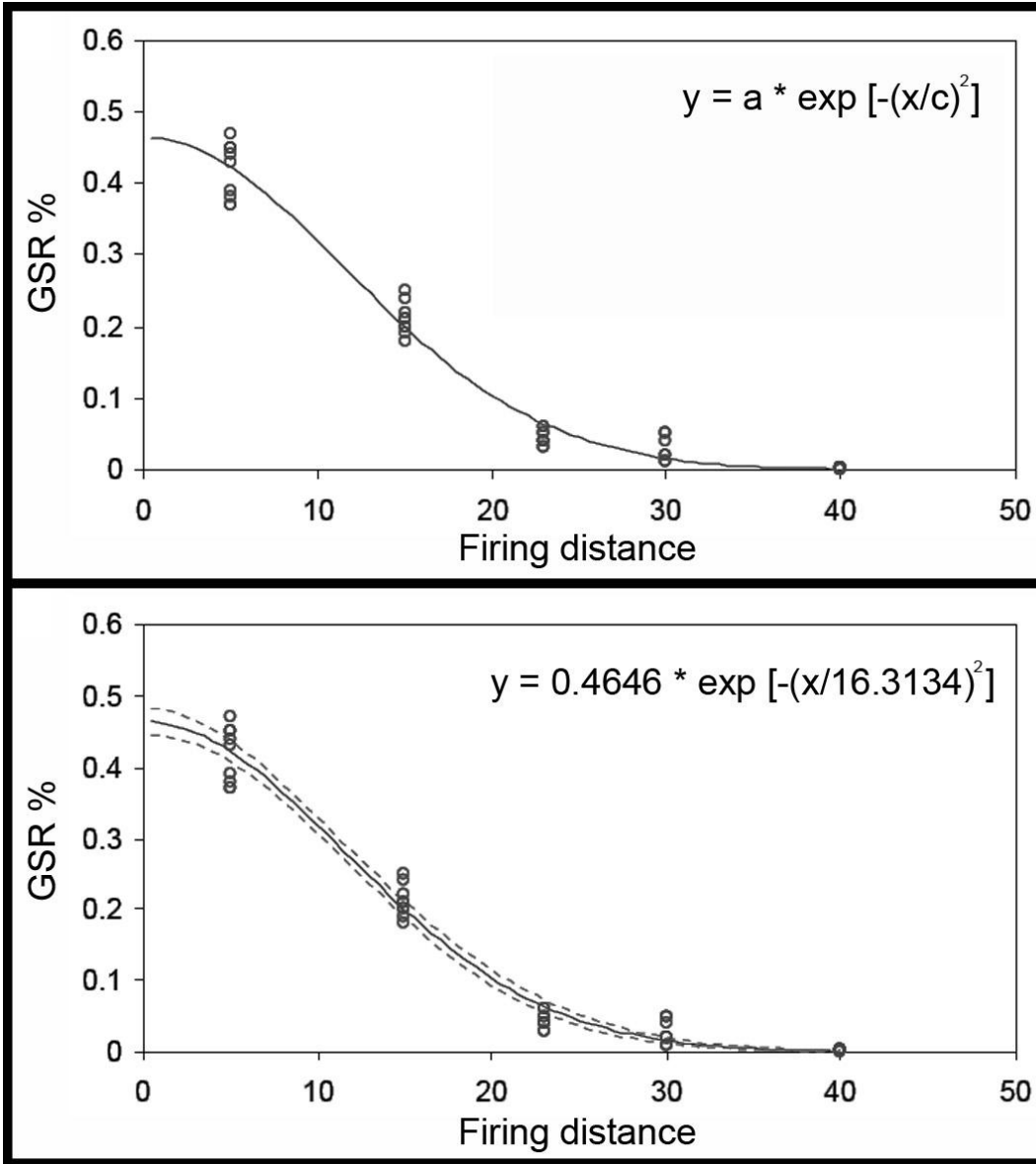


Figure 17. Graphs showing the Gaussian-like curve and its function, which were found to best fit the experimental data

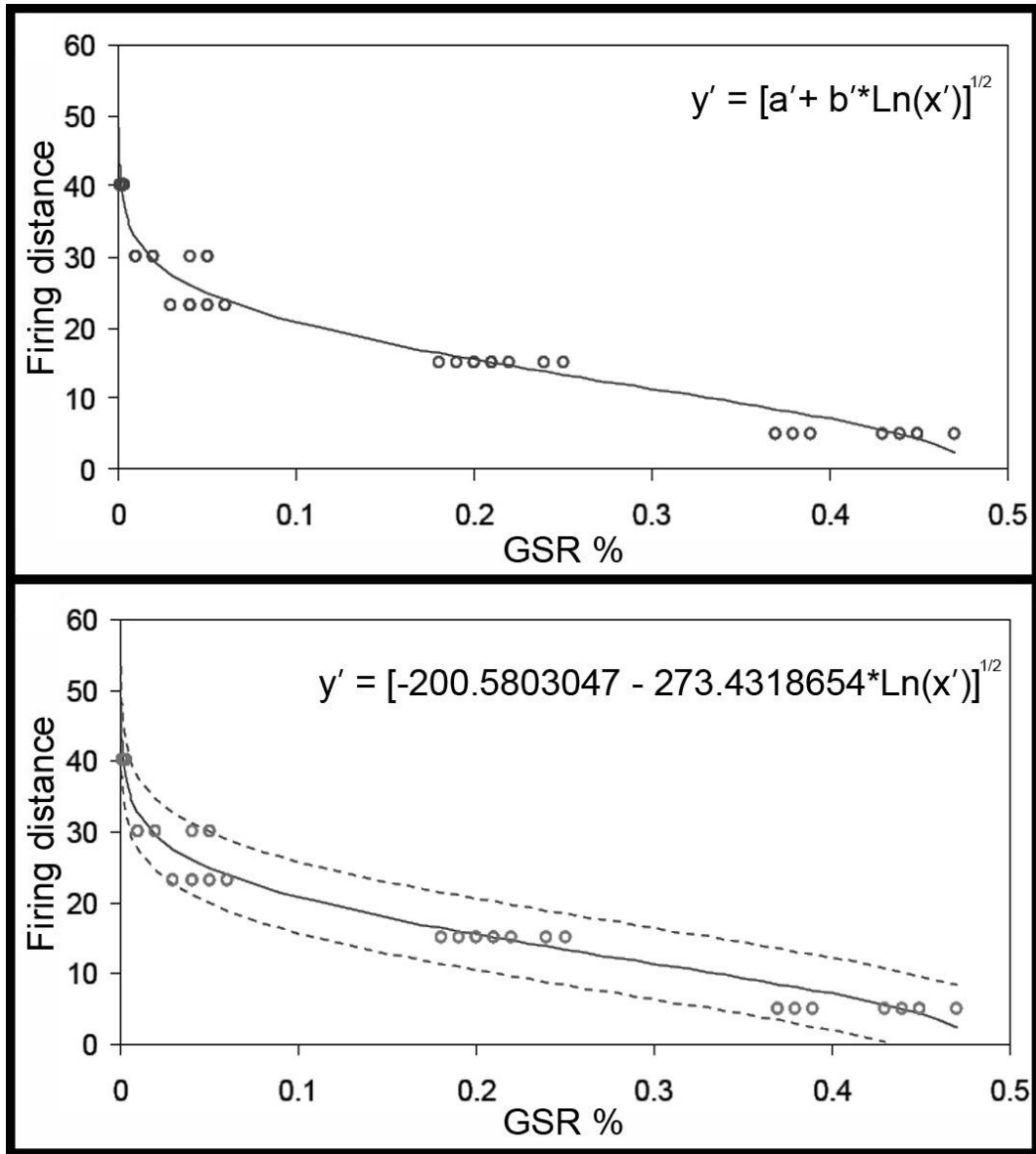


Figure 18. b. *Graphs showing the regression function estimated through a nonlinear regression analysis*

Table 3. *Estimation of the firing distance and its 95%CI given a known value of the GSR percentage (several calculation examples are reported)*

GSR %	Firing Distance	Lower 95%CI	Upper 95%CI
0.0001	48.1437	42.9363	53.3512
0.0005	43.3330	38.1632	48.5028
0.0010	41.0880	35.9343	46.2416
0.0050	35.3291	30.2130	40.4453
0.0100	32.5364	27.4362	37.6366
0.0500	24.8706	19.8059	29.9354
0.1000	20.7128	15.6612	25.7644
0.1500	17.8368	12.7909	22.8828
0.2000	15.4755	10.4312	20.5199
0.2500	13.3595	8.3132	18.4059
0.3000	11.3413	6.2880	16.3945
0.3500	9.2992	4.2300	14.3684
0.4000	7.0684	1.9588	12.1781
0.4500	4.2139	0	9.5046
0.4600	3.4274	0	8.8590
0.4700	2.4222	0	8.2522

Decomposed gunshot wounds

Macroscopic feature

Over the course of the experimental period of observation, characterized by skin slippage, powder particles and blackening became less visible and, consequently, the entrance wounds inflicted at different firing distances (5 cm, 15 cm, and 30 cm) became very similar at inspection, and difficult to be distinguished from the exit and stab wounds (Fig. 19).

Micro-CT feature

In decomposed samples the high-density particles ($> 1,000$ HU) were detected only in the dermis layer around the bullet track.

No GSR particles were detected in the exit holes and stab wounds (Fig. 19-20).

Histological feature

The skin of all samples showed extensive detachment of the epidermis; fungal colonies with focal hyphae were also evident.

Few of gunpowder interspersions were evident on the surface of the dermis layer of entry gunshot wounds (Fig. 19).

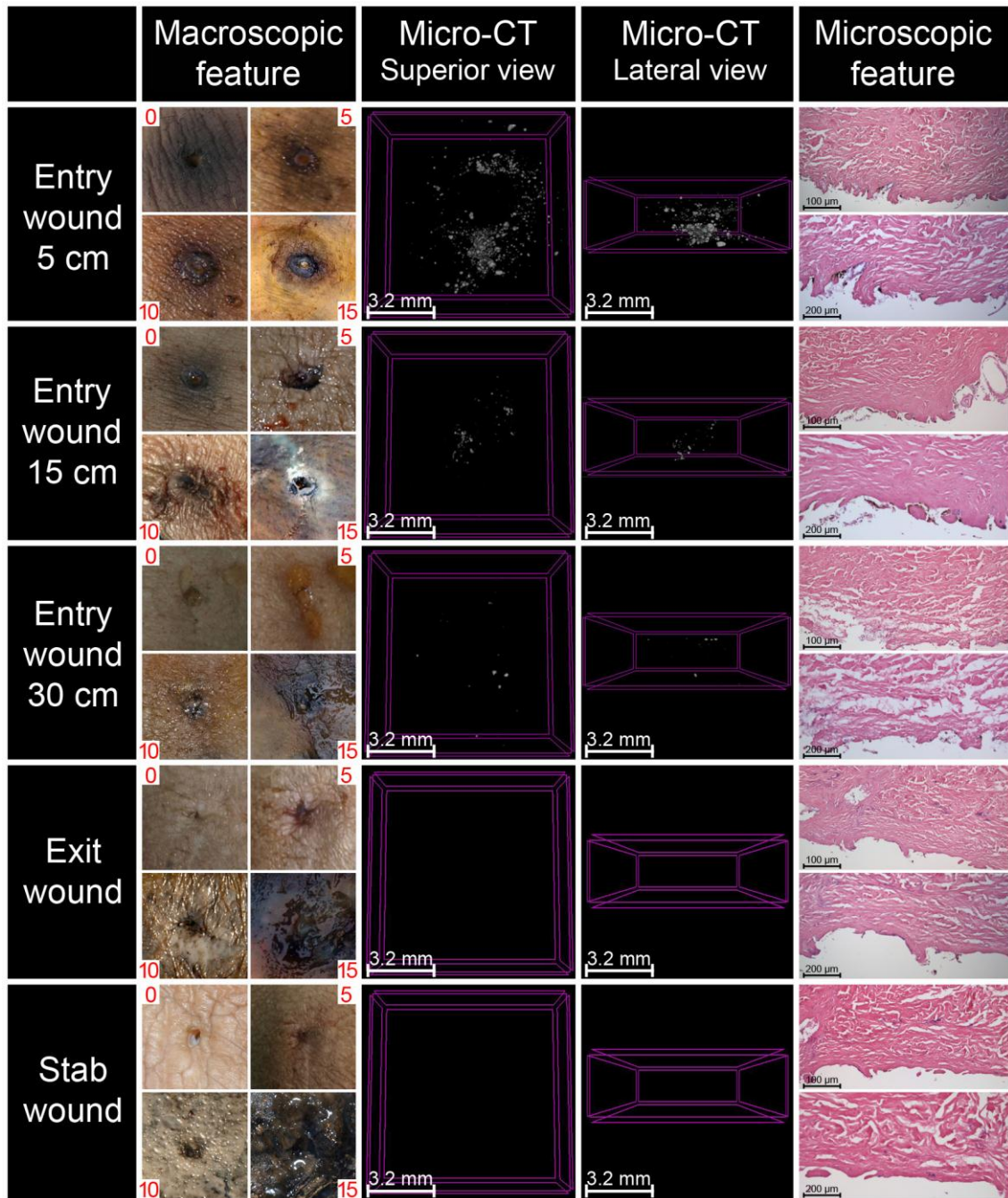


Figure 19. *Macroscopic, radiological and microscopic features of decomposed gunshot wounds*

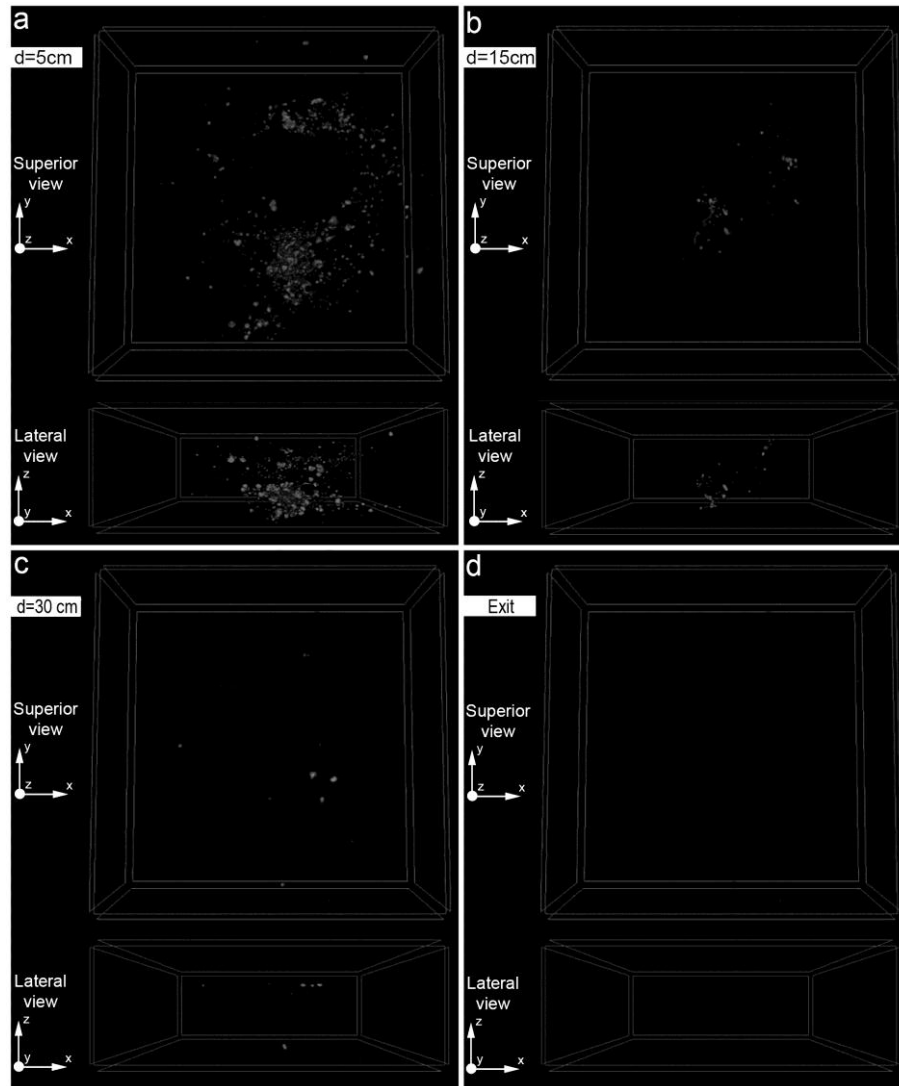


Figure 20. *3D reconstructions of decomposed gunshot wounds at different firing distances*

GSR amount

The mean percentages of GSR deposits for each tested firing distance are listed in Table n. 4.

The two-way ANOVA test showed that the mean percentage of GRS particles was significantly lower in decomposed than in fresh gunshot wounds ($p < 0.0001$) as well as among the different firing distances ($p < 0.0001$).

The post-hoc test with Bonferroni correction revealed that the amount of powder particles in decomposed samples was significantly higher in the wounds inflicted from 5 cm, than in those inflicted from 15 cm and 30 cm ($p < 0.0001$) (Fig. 21).

Table 4. *Results of the shooting trials.*

Analysis Variable: GSR percentage					
Firing range	Shots number	Mean	SD	Minimum	Maximum
Entry wound 5 cm	10	0,182	0.112	0.064	0.385
Entry wound 15 cm	10	0.021	0.008	0.009	0.040
Entry wound 30 cm	10	0.006	0.003	0.002	0.011
Exit wound	10	0.000	0.000	0.000	0.000
Stab wound	10	0.000	0.000	0.000	0.000

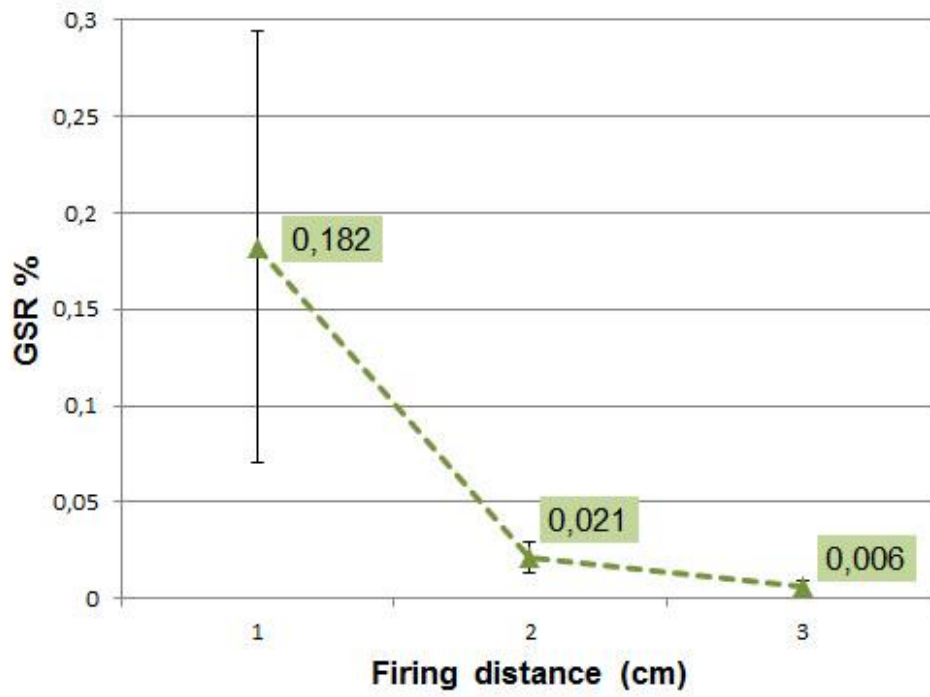


Figure 21. *Graphs showing the GSR concentrations detected by micro-CT analysis in decomposed gunshot wounds inflicted at different firing distances*

Charred gunshot wounds

Macroscopic feature

After the combustion process, the entrance wounds inflicted at different firing distances (5 cm, 15 cm, and 30 cm) became very similar at inspection because of the charring process of the skin with splitting of the epidermis. Consequently, it was impossible to differentiate them from the exit firearm wounds, and from the stab lesions (Fig. 22).

Micro-CT feature

The 3D reconstructions of each entrance gunshot wound showed the presence of radiopaque material with a density higher than 1,000 HU; however, the morphology of the entry hole and the bullet track was no more recognizable. In the firearm lesions inflicted at very close distance (5 cm), the GSR deposits were mainly constituted of huge particles ($> 150 \mu\text{m}$) with an irregular shape and well-delineated edges, while at greater distances (15 and 30 cm), agglomerates of tiny radiopaque particles scattered in the epidermis and dermis layers were evident.

No GSR deposits were detected in exit gunshot wounds and control specimens (stab lesions) (Fig. 22-23).

Histological feature

The skin of all samples showed peeling of the epidermis and intra- and subepidermal gap formation, with homogenization of the connective tissue fibers.

No gunpowder interspersions were evident on the surface of the dermis layer (Fig. 22).

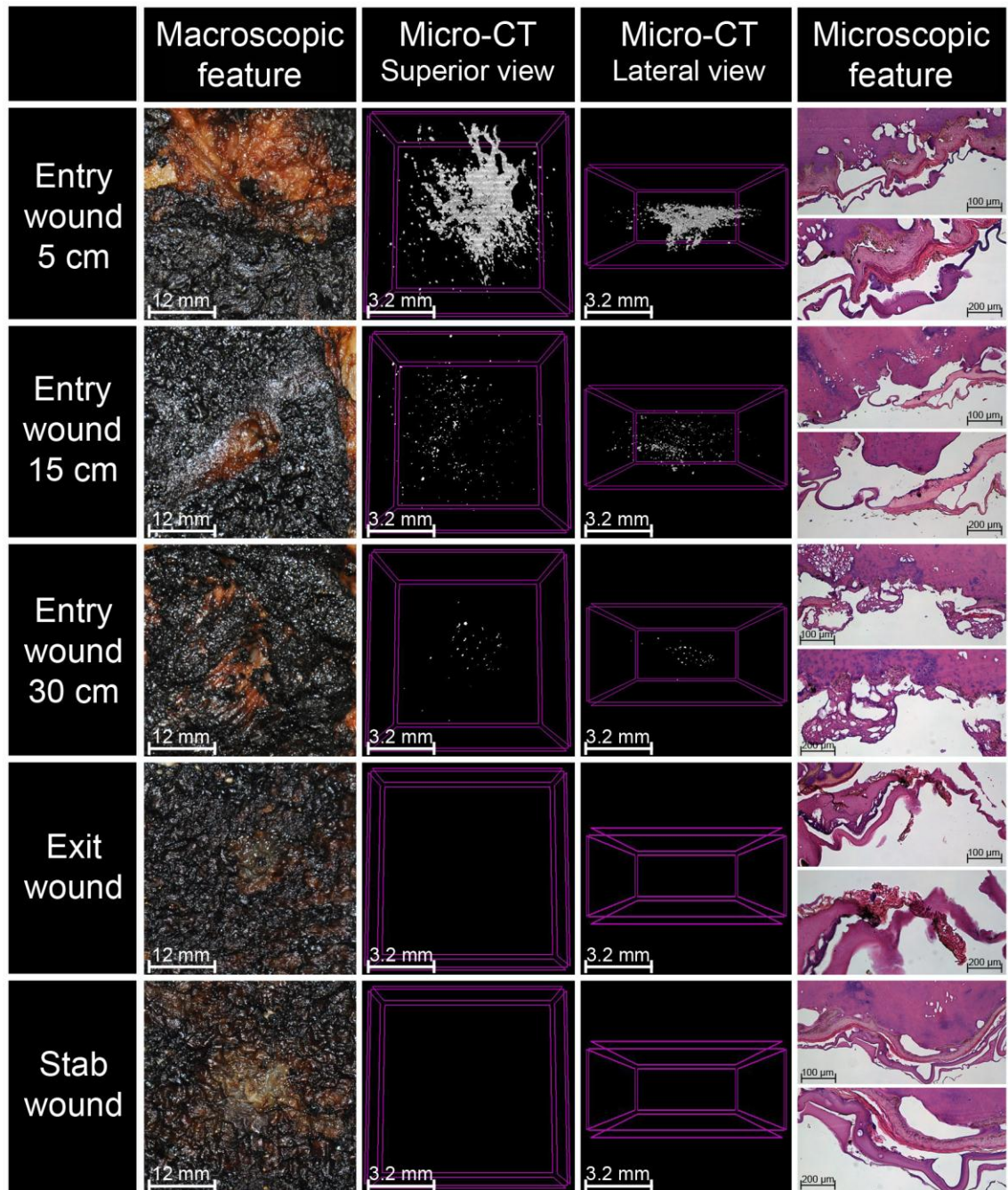


Figure 22. Macroscopic, radiological and microscopic features of charred gunshot wounds

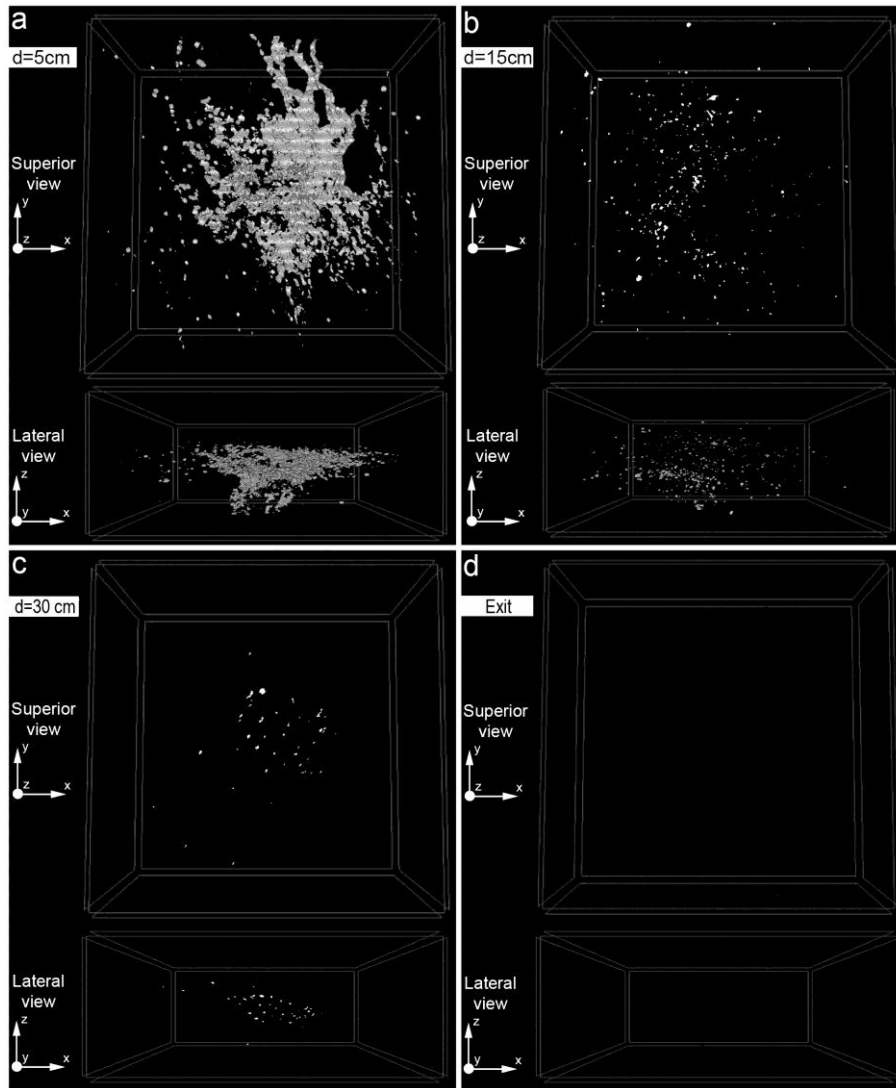


Figure 23. *3D reconstructions of charred gunshot wounds at different firing distances*

GSR amount

The mean percentages of GSR deposits for each tested firing distance are listed in Table n. 5.

The two-way ANOVA test showed that the mean percentage of GRS particles was significantly lower in charred than in fresh gunshot wounds ($p < 0.0001$) as well as among the different firing distances ($p < 0.0001$).

The post-hoc test with Bonferroni correction revealed that the amount of powder particles in charred samples was significantly higher in the wounds inflicted from 5 cm, than in those inflicted from 15 cm and 30 cm ($p < 0.0001$) (Fig. 24).

Table 5. *Results of the shooting trials.*

Analysis Variable: GSR percentage					
Firing range	Shots number	Mean	SD	Minimum	Maximum
Entry wound 5 cm	10	0,298	0.077	0.160	0.380
Entry wound 15 cm	10	0.014	0.004	0.011	0.019
Entry wound 30 cm	10	0.002	0.001	0.002	0.003
Exit wound	10	0.000	0.000	0.000	0.000
Stab wound	10	0.000	0.000	0.000	0.000

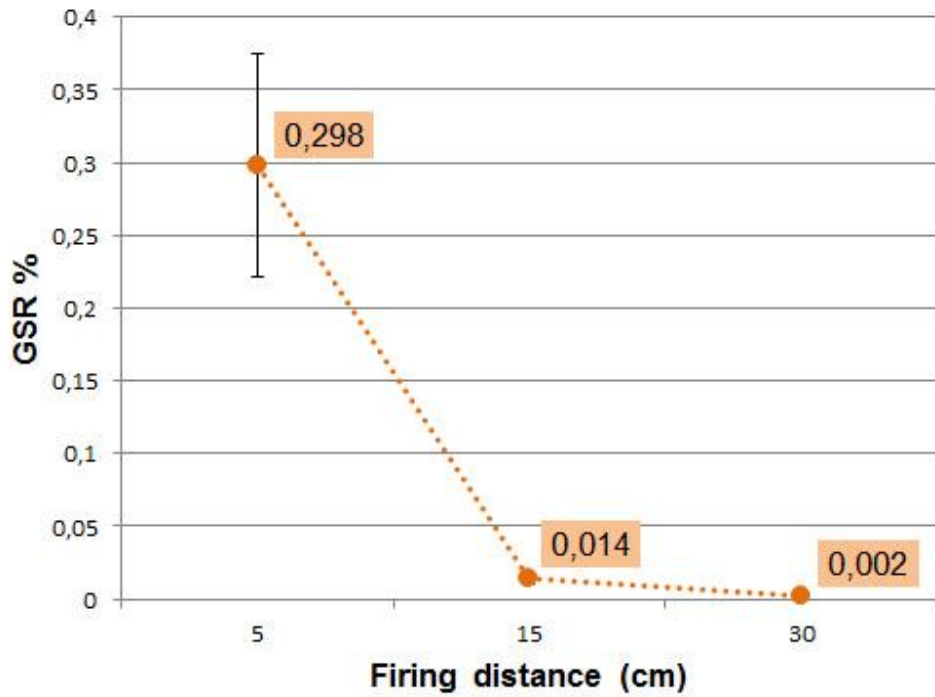


Figure 24. *Graphs showing the GSR concentrations detected by micro-CT analysis in charred gunshot wounds inflicted at different firing distances*

DISCUSSION

Experimental protocol

Gunshot residue analysis has been widely studied in the forensic literature for the estimation of the firing range [Dalby O et al, 2010].

The interplay between bullet and medium is highly complex, and takes place under exceptional physical conditions. For approximately 1 ms, decelerations of over 1 million m/s² and forces of well over 10,000 N are present. The physical characteristics of a material under such dynamic loads, especially the characteristics of biological structures, are virtually unknown. As a result, it would be difficult to produce a mathematical/physical model of the processes involved, and one would lack confidence in the results. Conducting experiments is therefore the only way to gain an understanding of the wounding process.

If such experiments are to produce a usable physical representation of real-life processes, they must fulfill a number of conditions [Kneubuehl BP et al, 2011]:

- the experiments must be reproducible and must always produce the same results;
- it must be possible to observe the process;
- bullet dynamics and the behaviour of the medium must correspond very closely to the real-life situation of a bullet in biological tissue;
- the values of the physical parameters along the wound channel (deceleration, force, penetration depth and timing) must be close to those encountered in real life.

Numerous experiments in various countries have resulted in the widespread adoption several materials for simulating soft tissue in wound ballistics experiments over the last few decades.

Gelatines, glycerine soaps or animal models (pig [Stein KM et al, 2000; Rainio J et al, 2003; Große Perdekamp M et al, 2005] or goat [Brown H et al, 1999], horse, and dog [Dalby O et al, 2010] have been mainly used as

simulants for wound ballistics. Each simulant has its advantages and disadvantages, and each has its role to play in wound ballistics experiments. For example, wounds in animals are not directly comparable to those in human beings because of the differences in the thickness and structure of the skin and the subcutaneous tissue, especially, in terms of retracting properties [Bartell TH et al, 1989]. Furthermore, the strength of the skin can have a significant effect on how the tip of the bullet deforms on contact with it, and hence on the behaviour of the bullet in the body; consequently, the entrance and exit holes may have a different morphology [Schantz B, 1979].

To avoid these limitations and disadvantages, we have elaborated a standardized experimental protocol using:

- human skin samples derived from surgically amputated calves;
- the same weapon (7.65 mm semi-automatic pistol - Beretta mod. 81);
- ammunitions from the same production lot (7.65x17 mm Browning SR full metal jacketed bullets);
- fixed stands with heights from 5 to 40 cm.

Even if, by definition, it is impossible to study the physiological reaction of a person to a bullet using a cadaver, we retain that this model is the best to study mechanical phenomena in the human body.

To obtain results similar from those obtained with a living person, the samples were kept frozen at -20°C until the day before the shooting experiments and then defrosted in open air for 12 hours. Moreover, all the experiments were carried out at ambient temperature.

Only intermediate-range gunshot wounds (5-40 cm) were investigated because when present they might offer critical information for reconstructing the dynamics of the event, above all when the issue of suicide, homicide and accidental firing is in question [Karger B et al, 2002].

Fresh gunshot wounds

In the last decades several techniques have been used for the detection and identification of GSR particles in intermediate-range gunshot wounds [Dalby O et al, 2010]. These experiments have clarified that the amount and spatial distribution of GSR on the skin surrounding the entrance wound is strictly correlated to the shooting distance [Brown H et al, 1999; Neri M et al, 2007].

Noteworthy are the results obtained by Brown et al who performed a statistical analysis of the relationship between the firing range and the amount and distribution of GSR deposits in firings below 45 cm performed on pig skin. Using Alizarin Red S staining and automated image analysis software the authors showed a decreasing trend in the mean GSR area by increasing the firing distance. In addition they found that GSR particles were heavily concentrated in the wound tract only for contact and close range shots at 2.5 cm, while the particle distribution was more uniform between the wound tract and the skin surfaces for shots fired from more than 2.5 cm [Brown H et al, 1999].

Our results, obtained scanning the entire entrance wound by means of a micro-CT system coupled to image-analysis software, confirm the findings by Brown et al, clearly showing that, in intermediate-range gunshot wounds, the amount of GSR resulting from the discharge of the firearm is dependent in a non-linear fashion on the distance from which the gun was fired. Indeed, using a curve fitting process, a Gaussian model was found to best describe the relationship between the firing distance (independent variable “x”) and the GSR percentage (dependent variable “y”), with $R^2 = 0.9876$ (Fig. 17).

Although histochemistry [Tschirhart DL et al, 1991; Brown H et al, 1999; Marty W et al, 2002; Neri M et al, 2007, Andreola S et al, 2011] and electron microscopy methods [Ueyama m et al, 1980; Amadasi A et al, 2012] are accurate and precise for estimating the firing distance, they

require a labour intensive exercise, because each specimen has to be cut into several sections, and each section requires a microscopic analysis.

On the contrary, in our work the entrance wound was cut into a single cube (edge length=1 cm), formalin fixed, and scanned with a Micro-CT system. This procedure, which is less time-consuming and expensive than histochemistry or electron microscopy, allowed to simultaneously analyse the epidermidis and dermis around and inside the entrance hole and to perform tri-dimensional reconstructions of the spatial distribution of the GSR particles, permitting a gross optical discrimination between shots fired from distances greater than 30 and those from 23 cm or less.

Moreover, statistical analysis found significant differences in the amount of powder residue deposited on the skin at each tested firing distance (Fig. 16-17). Based on the Gaussian function ($y' = [-200.5803047 - 273,4318654 * \text{Ln}(x')]^{1/2}$) it was possible to estimate the firing distance (expressed as a 95% CI of values) given a known percentage of the GSR deposit (Fig. 18). For example, a GSR% of 0.15% corresponds to a firing distance of 17.8 cm (95%CI 12.8 cm – 22.9 cm) (Table n. 3). Obviously, to reduce the size of the firing range corresponding to a single GSR deposit, the shootings experiments for each distance and the number of tested distances should be increased.

The potential effect of the material picked up by the bullet during its passage through the bore and left on the skin of the entrance hole (bullet wipe) on the variability of the GSR amount for a specific firing distance has been described also for full metal jacketed bullets [Kijewski H et al, 1993; Berryman HE et al, 2010].

In our study, however, no specific experiments were carried out in order to quantify the percentage of deposits referable to the bullet wipe mark.

Since the relationship between the distribution and the amount of firearm discharge residue associated with a gunshot wound depends on several variables [Brozek-Mucha Z et al, 2001; Große Perdekamp M et al, 2005],

micro-CT analysis might be of practical use only if experiments are conducted scanning both the victim's gunshot entrance holes, and a minimum number of experimental wounds produced on human skin samples (i.e. 10 replicates for each firing distance).

Moreover, when the weapon is not found during the crime investigation, or the bullets are not collected at the autopsy, it is fundamental that an equivalent type of firearm and ammunition (or at least a gun of the same calibre) are used during the experimental shootings, in order to control the variables related to the type of firearm [Brozek-Mucha Z et al, 2001; Große Perdekamp M et al, 2005].

Analysing the 3D-reconstructions, GSR deposits were detected on the entrance gunshot wounds of all the tested firing distances (Fig. 15a-e), while the exit lesions did not present any particles with a density higher than 1,000 HU (Fig. 15f).

In a recent paper, Perdekamp et al. have demonstrated that in contact shots fired against composite pig skin-gelatine models, GSR particles were detectable also in the distal sections of the missile track up to the exit hole, while in our study no GSR particles were visible within and around the exit holes [Große Perdekamp M et al, 2011].

These apparent divergences might have been caused by the different experimental models used (composite pig skin-gelatine model vs. human calf sections) and by the longer muzzle-to-target distances tested in our study (5, 15, and 30 cm), which probably avoided the massive invasion of combustion products along the wound track.

Decomposed gunshot wounds

Decomposition and burial can obscure obvious GSR tattooing or stippling, while insect or other animal activity can create new tracts, obscure existing tracts, and subsequently change the morphology of the wound [Pollak S et al, 1988]. Hence, in cases of badly preserved corpses, the identification of gunshot wounds may be difficult to perform macroscopically.

Previous experimental studies on animals, in which intermediate-range gunshot wounds were produced and macro/microscopically observed after a period of decomposition on air for several days, have been reported [Gibelli D et al, 2010; MacAulay LE et al 2009; LaGoo L et al, 2010; Udey RN et al, 2011].

MacAulay et al. have macroscopically examined putrefied gunshot wounds inflicted on pigs at three different ranges (contact, 2,5 cm, and 1,75 m), concluding that changes due to decomposition (tested conditions: 14 days of observation period, temperature ranging between 7°C and 22°C) did not affect the collection and interpretation of gunshot wound evidence until the skin was degraded in the late active or advanced decay stage of decomposition [MacAulay LE et al 2009].

Similar macroscopic results were obtained by Gibelli et al with a 16 week-period of observation; however, the authors detected lead and antimony in degraded tissues by means of histological analysis (sodium rhodizonate test) and radiochemical investigation (neutron activation analysis), respectively [Gibelli D et al, 2010].

On the other hand, LaGoo et al observed that blackened wound edges and GSR particle deposition inside and around the entrance wound could not be macroscopically distinguished after a period of 7 summer days (range of temperature: 1.8 - 31,4°C). Analysing microwave-digested wound samples by ICP-MS, the same authors detected antimony, barium, and lead particles at measurable levels throughout the entire sampling period (35 days), concluding that the presence and amount of GSR in tissues samples was

more dependent on the decomposition stage rather than the time since the wound was inflicted [LaGoo L et al, 2010]. In a further study, it was demonstrated that ICP-MS analysis of close-range gunshot wounds has the ability to differentiate the GSR particles originated from shots fired with two different bullet types (jacketed vs. nonjacketed), in both fresh and decomposed samples [Udey RN et al, 2011].

Since all the above-mentioned experiments were conducted on animal models, our purpose was to assess the effects of early stages of decomposition on gunshot wounds produced on human samples.

In our experiments, fresh entrance wounds exhibited typical characteristics of intermediate gunshot wounds (i.e. powder particles and blackening), being easily distinguishable from the exit holes (Fig. 19 – day 0). After 15 days at open air, with an average temperature of 24,5°C and an average humidity of 64,9%, the decomposition activities altered the skin surface, hampering the macroscopic differential diagnosis between entry and exit wounds (Fig. 19 – day 15).

The ANOVA test confirmed the results of Lagoo et al proving a statistically significant difference between the amount of powder particles detected in fresh and decomposed samples.

Additionally, in fresh entrance wounds, the 3D reconstructions (lateral view) revealed particles with a density higher than 1,000 HU in the epidermis and dermis layers of the skin around the hole, while in decomposed samples only the particles deeply penetrated into the dermis layer were evident (Fig. 25). T

hese findings may be explained by the post-mortal detachment of the epidermis (Fig. 19), which could have caused the loss of the GSR particles deposited on the skin surface.



Figure 25. *3D reconstructions of fresh and decomposed samples*

Also in decomposed gunshot wounds, the amount of GSR roughly correlated in a non-linear fashion with the distance from which the gun was fired. However, in contrast to fresh samples, a high variability of the GSR values estimated for shots repeatedly fired from the same distance was observed, particularly at very close range (5 cm) (Fig. 26). We believe that this variability could have been partly caused by the differences in the thickness and structure of the skin of the utilized human calves, which can significantly influence skin putrefaction and autolysis of the tissue [Janssen W, 1984].

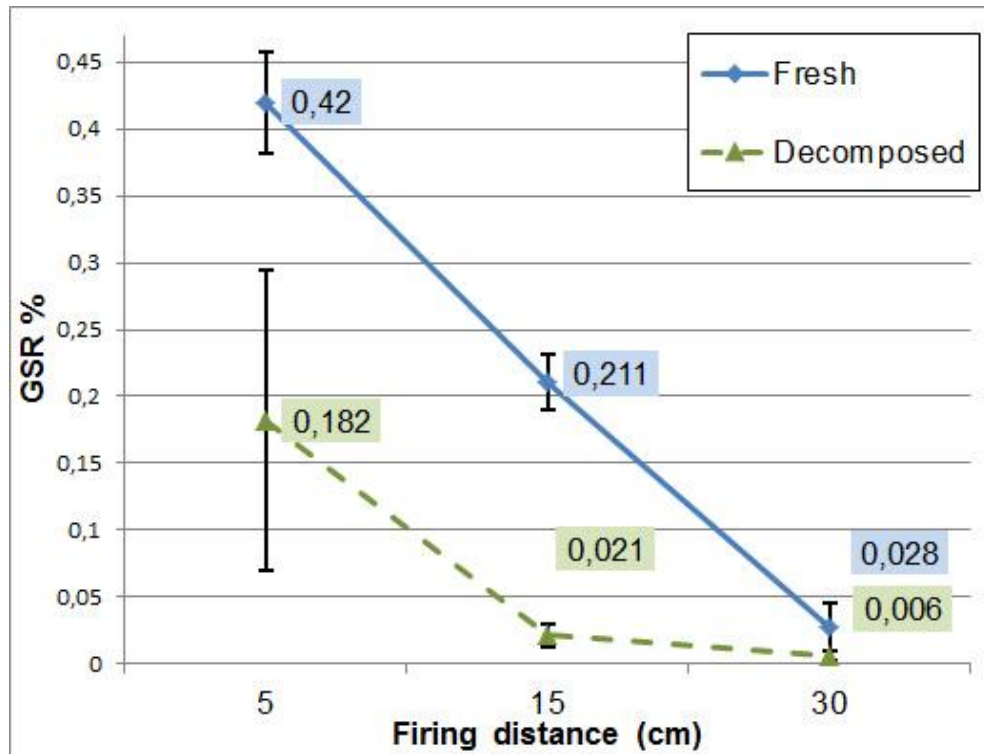


Figure 26. *Graphs showing the GSR concentrations detected by micro-CT analysis in fresh and decomposed gunshot wounds*

It is well-known that decomposition is a progressive process affected by several intrinsic and extrinsic factors, such as carrion insects abundance, temperature, humidity, rainfall, and exposure [Spitz WU et al, 1973]. As reported above, micro-CT analysis might be of practical use for estimating the firing range, but a series of shooting trials should be carried out using human skin samples with the same, or at least an equivalent type of weapon and ammunition, in order to control the variables related to the type of firearm used. Given the high variability of the results we have obtained on decomposed wounds even under standardized environmental conditions (i.e. site, time, temperature, and humidity), and considering that in forensic practice it is generally very hard to determine the exact moment when the gunshot wound was inflicted, and to reproduce the same conditions of exposure from death until the retrieval of the corpse, we retain that the analysis of GSR through micro-CT, as well as other quantitative techniques, should not be used for estimating the firing range in decomposed wounds.

Charred gunshot wounds

When gunshot wounds are found in a charred corpse it is always necessary to determine the manner of death, comparing all the available findings to typical characteristics of suicide or homicide [Copeland AR, 1985]. Indeed, even if burning can be often employed in cases of firearm homicide to destroy forensic evidence or to prevent victim's identification [Ubelaker DH, 2009], in rare cases of complex suicide by shooting and subsequent self-immolation [Türk EE et al, 2004; Adair TW et al, 2006, Bohnert M et al, 2003], when the victims want to protect themselves against failure of the first method or intend to burn their mortal remains so that their depart from this world is complete [Türk EE et al, 2004], have been described in the literature.

Specific autopsy findings, such as the number and site of the entrance wounds, the shooting distance, and the direction of the internal bullet path are crucial elements for the reconstruction of the manner of death. A combination of the above-mentioned typical findings can represent strong evidence for suicide or homicide, whereas "atypical patterns" should ring an alarm and suggest the necessity of a more in-depth examination [Karger B et al, 2002]. Unfortunately, in charred bodies, the surface of wounds can be distorted or obliterated by the effect of fire [Dettmeyer RB et al, 2011]. Furthermore, many authors have emphasized the importance of recognizing artifactual changes in burned bodies that may simulate ante-mortem injuries [Pope EJ et al, 2004; Hausman R et al, 2002; Tsokos M et al, 2011]. Splittening of the skin, characterized by sharp edges, often involving the subcutaneous fatty tissue and sometimes the outer muscle layer, is a frequently observed phenomenon. These post-mortem lesions, caused by a heat-related shrinkage of the skin or by the manipulation of the body while recovering it and putting it into the coffin, may be erroneously interpreted as vital injuries [Bohnert M, 2004]. Pre-autopsy X-rays can be useful for the identification of bullets, metallic parts from the primer or the cartridge

case, knife blade tips, and other features that might clarify the nature of any trauma sustained [Dolinak D et al, 2008; Stein KM et al, 2000, Ruttly GN et al, 2008]. Recently, Amadasi et al, analysing 31 adult bovine ribs shot at near-contact with a single bullet, and subsequently exposed to a “charring cycle”, have demonstrated the survival of GSR even after an extreme fire alteration, showing that metallic residues can be detected in charred bones by conventional radiological investigations [Amadasi A et al, 2011] and/or environmental scanning electron microscopy (SEM-EDX) [Amadasi A et al, 2012].

It is largely agreed in the forensic literature that it is hardly possible to completely destroy a body [Bohnert M et al, 1998]. Indeed, in the majority of cases, when a corpse undergoes a burning process, a certain amount of soft tissue is preserved [Bohnert M et al, 2003]. For this reason, in our study, the applied temperature and the duration of the exposure of the calves to the open flames were optimized for producing fourth-degree burns (characterized by charring of the skin with splitting of the epidermis), and not for the complete destruction of the biological sample. Regarding ammunitions, we have utilised full metal-jacketed bullets because it is well known that these kinds of projectiles leave less GSR in the tissues, making it more difficult to precisely locate the entrance wound in a charred body [Amadasi A et al, 2011]. After the experimental burnings, we have observed the impossibility to macroscopically and/or microscopically differentiate the entry gunshot wounds from the exit holes and the stab lesions (Fig. 22). Additionally, new circular holes produced by the splitting of the epidermidis could be noticed.

Micro-CT analysis, performed scanning the entire wound (epidermis and dermis around and inside the wound track), clearly showed the presence of radiopaque material with a density higher than 1,000 HU in each entrance gunshot wound, while the exit and stab lesions did not present any metal particles. In wounds shot at a distance of 5 cm, the 3D high-resolution

reconstructions revealed spherical particles with a huge size (diameter $> 150 \mu\text{m}$) and an irregular shape similar to those described in charred firearm wounds using different analytical techniques [Dolinak D et al, 2008; Amadasi A et al, 2012]. An interesting datum was that, because of the shrinkage of the subcutaneous tissue, neither macroscopically nor by micro-CT could the wound tracks be visualised in charred samples (Fig. 27).



Figure 27. 3D reconstructions of fresh and charred samples

Given the high temperatures reached during the charring process, it may be hypothesised a melting of the neighbouring metal residues with a consequent aggregation of the particles. This phenomenon was not observed in the wounds shot from 15 and 30 cm, probably because the lower amount of GSR and the scattering of the particles in the epidermis and dermis layers at these firing distances prevented the confluence of the metal residues, which appeared as minute isolated fragments.

The statistically significant decrease in the total amount of powder particles in charred samples compared with fresh samples could be ascribed to the burning process (Fig. 28). However, despite the loss of residues and the other fire-related alterations of the samples, the decreasing trend in the mean GSR area by increasing the firing distance was confirmed also for the charred firearm wounds.

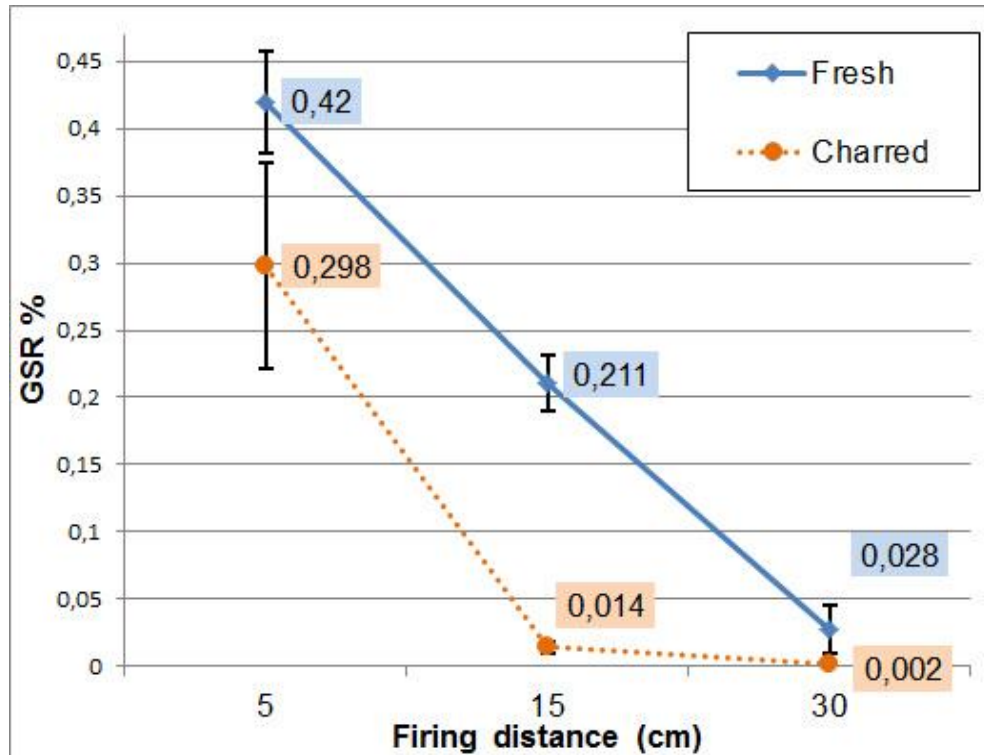


Figure 28. Graphs showing the GSR concentrations detected by micro-CT analysis in fresh and charred gunshot wounds

Key-points to further investigate are the roles of temperature and duration of fire exposure in the reduction of the quantity of GSR in charred samples. Analysing both 3D-recostructions and histology the decrease in the total number of residues appears partly linked to the global volatilization of the constituents of the GSR (present as oxides in the propulsive charges) [Amadasi A et al, 2012], and mainly due to the fire-related destruction of the superficial layers of the skin (Fig. 22), as observed also in decomposed samples (Fig. 19).

Limits of the research

The present method exhibits the limits discussed below.

First, micro-CT analysis gives an indirect identification of GSR particles; thereby, substances with the same density of powder particles might be erroneously tagged as GSR, generating a false positive result. Considering that micro-CT is a non-destructive technique [Cnudde V et al, 2008], a possible solution for the above-mentioned problem could be the identification of the chemical composition of the metal residues by means of a “*gold-standard*” method, such as ESEM coupled with an EDS [Viel G et al, 2009; Amadasi A et al, 2012], ICP-MS [Udey RN et al, 2011] and/or NAA [Poppa P et al, 2011; Gibelli D et al, 2010], thus strongly reducing the possibility of a misinterpretation of the results.

Another limit might be the decision to calculate the percentage of GSR excluding all the particles with a density lower than 1000 HU; this implies that a range of light metal alloys could not be detected as GSR deposits. However, in order to determine the firing distance, a precise quantification of the real amount of the particles is probably not as important as the measurements of the relative variations in the amount of GSR between different firing distances.

CONCLUSIONS

Our study, which is the first application of micro-CT analysis in the field of forensic ballistics, demonstrates that this radiological technique could be an objective, rapid, and non-destructive tool for the analysis of gunshot wounds in firearm fatalities.

On fresh samples, this method may be of practical use for estimating the firing range given a known percentage of the GSR deposit.

Regarding the analysis of gunshot wounds in bodies in advanced decomposition or extremely damaged by fire, the micro-CT analysis might furnish precious information on nature and means of productions of an injury, supporting the differential diagnosis between gunshot and sharp-force wounds, entry and exit holes, and ante-mortem and post-mortem lesions.

Indeed, this high-resolution tomographic technique, capable of detecting metal particles also in intermediate-range gunshot wounds extremely altered by post-mortem phenomenon, could be easily and quickly used as a screening test for the analysis of suspected wounds and, in combination with other autopsy and crime scene findings, play an important role for reconstructing the shooting incident.

For estimating the sensitivity and specificity of the proposed method, it will be necessary to test the micro-CT analysing specimens of forensic caseworks and to confirm the positive results with a “*gold-standard*” method, such as:

- ESEM- EDX [Viel G et al, 2009; Amadasi A et al, 2012];
- ICP-MS [Udey RN et al, 2011];
- NAA [Poppa P et al, 2011; Gibelli D et al, 2010].

Finally, since the relationship, between the distribution and the amount of firearm discharge residue associated with a gunshot wound, depends on several variables, future development may consist in extending this method to other shot trials:

- a) using different type of weapons (pistol, revolver, rifle) and bullets (lead and jacketed);
- b) analyzing samples altered by the effects of water or snow;
- c) changing the conditions of the target.

REFERENCES

- Adair TW, Fisher A. Suicide with associated acts of arson: two cases from Colorado. *J Forensic Sci* 2006;51:893–5.
- Aleksandar I. Is there a way to precisely identify that the suspect fired from the firearm? *Forensic Sci Int* 2003;136(Suppl. 1):158–9.
- Amadasi A, Borgonovo S, Brandone A, Di Giancamillo M, Cattaneo C. The survival of metallic residues from gunshot wounds in cremated bone: a radiological study. *Int J Legal Med* 2011 [Epub ahead of print]
- Amadasi A, Brandone A, Rizzi A, Mazzarelli D, Cattaneo C. The survival of metallic residues from gunshot wounds in cremated bone: a SEM-EDX study. *Int J Legal Med* 2012 [Epub ahead of print].
- Andreola S, Gentile G, Battistini A, Cattaneo C, Zoja R. Forensic applications of sodium rhodizonate and hydrochloric acid: a new histological technique for detection of gunshot residues. *J Forensic Sci* 2011;56:771-4.
- Bartell TH, Mustoe TA. Animal models of human tissue expansion. *Plast Reconstr Surg* 1989;83:681–6.
- Basu S. Formation of gunshot residues. *J Forensic Sci* 1982;27:72–91.
- Berryman HE, Kutyla AK, Davis RJ 2nd. Detection of gunshot primer residue on bone in an experimental setting—an unexpected finding. *J Forensic Sci* 2010;55:488–491.
- Bohnert M. Morphological Findings in Burned Bodies. In: Tsokos M (ed) *Forensic Pathology Reviews Volume 1*. 2004; Humana Press, Totowa:3–27.
- Bohnert M, Rost T, Pollak S. The degree of destruction of human bodies in relation to the duration of the fire. *Forensic Sci Int* 1998;95:11–21.
- Bohnert M, Rothschild MA. Complex suicides by self-incineration. *Forensic Sci Int* 2003;131:197–201.

- Bohnert M, Werner CR, Pollak S. Problems associated with the diagnosis of vitality in burned bodies. *Forensic Sci Int* 2003;135:197–205.
- Brown H, Cauchi DM, Holden JL, Allen FC, Cordner S, Thatcher P. Image analysis of gunshot residue on entry wounds. II – A statistical estimation of firing range. *Forensic Sci Int* 1999;100:179–86.
- Brown H, Cauchi DM, Holden JL, Wrobel H, Cordner S. Image analysis of gunshot residue on entry wounds. I – The technique and preliminary study. *Forensic Sci Int* 1999;100:163–77.
- Brozek-Mucha Z, Jankowicz A. Evaluation of the possibility of differentiation between various types of ammunition by means of GSR examination with SEM-EDX method. *Forensic Sci Int* 2001;123:39–47.
- Can M, Uner HB, Koc S, Tok M, Disbudak M. Determination of hand deposited gunshot residue obtained from shootings carried out with handgun cartridges produced by Turkish machinery and chemistry foundation using flameless atomic absorption spectrophotometer. *Forensic Sci Int* 2003;136(Suppl. 1):147.
- Capannesi G, Sedda F. Bullet identification: a case of a fatal hunting accident resolved by comparison of lead shot using instrumental neutron activation analysis. *J Forensic Sci* 1992;37:657–62.
- Cnudde V, Masschaele B, De Cock H, Olstad, Vlaminck L, Jacobs P. Virtual histology by means high resolution X-ray CT. *Journal of Microscopy* 2008;232:476–85.
- Cooper R, Guileyardo JM, Stone IC, Hall V, Fletcher L. Primer residue deposited by handguns. *Am J Forensic Med Pathol* 1994;15:325–7.
- Copeland AR. Homicide by fire. *Z Rechtsmed* 1985;95:59–65.
- Dalby O, Butler D, Birkett JW. Analysis of gunshot residue and associated materials--a review. *J Forensic Sci* 2010;55:924–43.

- Dettmeyer RB. Forensic Histopathology. Fundamentals and Perspectives. 2011; Springer-Verlag Berlin Heidelberg New York.
- Di Maio VJM. Gunshot wounds. Practical aspects of firearms, ballistics, and forensic techniques. 1999; CRC Press, Boca Raton, London, New York, Washington D.C.
- Dolinak D, Wise SH, Jones C. Microscopic and spectroscopic features of gunpowder and its documentation in gunshot wounds in charred bodies. *Am J Forensic Med Pathol* 2008;29:312–9.
- Germani MS. Evaluation of instrumental parameters for automated scanning electron-microscopy / gunshot residue particle analysis. *J Forensic Sci* 1991;36:331–42.
- Gibelli D, Brandone A, Andreola S, Porta D, Giudici E, Grandi MA, Cattaneo C. Macroscopic, Microscopic, and Chemical Assessment of Gunshot Lesions on Decomposed Pig Skin. *J Forensic Sci* 2010;55:1092–7.
- Große Perdekamp M, Vennemann B, Mattern D, Serr A, Pollak S. Tissue defect at the gunshot entrance wound: what happens to the skin? *Int J Legal Med* 2005;119:217–22.
- Große Perdekamp M, Arnold M, Merkel J, Mierdel K, Braunwarth R, Kneubuehl BP, Pollak S, Thierauf A. GSR deposition along the bullet path in contact shots to composite models. *Int J Legal Med* 2011;125:67–73.
- Hausmann R, Betz P. Thermally induced entrance wound-like defect of the skull. *Forensic Sci Int* 2002;128:159–61.
- Janssen W. Forensic Histopathology. 1984; Springer Verlag, Berlin, Heidelberg, New York, Tokyo.
- Karger B. Forensic ballistic. In: Tsokos M (ed) *Forensic Pathology Reviews Volume 5*. 2008; Humana Press, Totowa:139–72.

- Karger B, Billeb E, Koops E, Brinkmann B. Autopsy features relevant for discrimination between suicidal and homicidal gunshot injuries. *Int J Legal Med* 2002;116:273–8.
- Kijewski H, Bock G. Veränderungen der Sb- und Pb-Konzentration im Abstreifring bei Schüssen mit Langwaffen aus Entfernungen bis 400 m. *Beitr Gerichtl Med* 1993;41:383–9.
- Kneubuehl BP, Coupland RM, Rothschild MA, Thali MJ. *Wound Ballistics. Basics and Applications*. 2011; Springer-Verlag Berlin Heidelberg New York.
- Koons RD, Havekost DG, Peters CA. Analysis of gunshot primer residue collection swabs using flameless atomic-absorption spectrophotometry; a reexamination of extraction and instrument procedures. *J Forensic Sci* 1987;32:846–65.
- Koons RD, Havekost DG, Peters CA. Determination of barium in gunshot residue collection swabs using inductively coupled plasma-atomic emission-spectrometry. *J Forensic Sci* 1988;33:35–41.
- Koons RD. Analysis of gunshot primer residue collection swabs by inductively coupled plasma-mass spectrometry. *J Forensic Sci* 1998;43:748–54.
- Koons RD. Flameless atomic-absorption spectrophotometric determination of antimony and barium in gunshot residue collection swabs—a collaborative study. *Crime Lab Dig* 1993;20:19–23.
- Krishnan SS. Firing distance determination by atomic absorption spectroscopy. *J Forensic Sci* 1974;19:351–86.
- Krishnan SS. Detection of gunshot residue on the hands by neutron activation and atomic absorption analysis. *J Forensic Sci* 1974;19:789–97.
- Krishnan SS. Firing distance determination by atomic absorption spectrophotometry. *J Forensic Sci* 1974;19:351–6.

- Krishnan SS. Firing distance determination by neutron activation analysis. *J Forensic Sci* 1967;12:471–83.
- LaGoo L, Schaeffer LS, Szymanski DW, Waddell Smith R. Detection of Gunshot Residue in Blowfly Larvae and Decomposing Porcine Tissue Using Inductively Coupled Plasma Mass Spectrometry (ICP-MS). *J Forensic Sci* 2010;55:624–32.
- Lebiedzki J, Johnson DL. Handguns and ammunitions indicators extracted from the GSR analysis. *J Forensic Sci* 2002;47:483–93.
- MacAulay LE, Barr DG, Strongman DB. Effects of Decomposition on Gunshot Wound Characteristics: Under Moderate Temperatures with Insect Activity. *J Forensic Sci* 2009;54:443–7.
- Marty W, Sigrist T, Wyler D. Determination of firing distance using the rhodizonate staining technique. *Int J Legal Med* 2002;116:1–4
- Matty W. Primer composition and gunshot residue. *Assoc Firearms Tool Mark Exam J* 1982;19:8–13.
- Meng HH, Caddy B. Gunshot residue analysis—a review. *J Forensic Sci* 1997;42:553–70.
- Morales EB, Vazquez ALR. Simultaneous determination of inorganic and organic gunshot residues by capillary electrophoresis. *J Chromatogr A* 2004;1061:225–33.
- Nag NK, Sinha P. A note on assessability of firing distance from Gunshot Residues. *Forensic Sci Int* 1992;56:1–17.
- Neri M, Di, Turillazzi E, Riezzo I, Fineschi V. The determination of firing distance applying a microscopic quantitative method and confocal laser scanning microscopi for detection of gunshot residue particles. *Int J Legal Med* 2007;121:287–92.
- Pillay KKS, Jester WA, Fox HA. New method for the collection and analysis of gunshot residues as forensic evidence. *J Forensic Sci* 1974;19:768–83.

- Pluisch F, Sellier K. Führt der Beschuß von Knochen mit Reinblei-KK-Geschossen zu Metallabrieb? Arch Kriminol 1994;194:155–60.
- Pollak S, Reiter C. Maggot-induced postmortem changes simulating gunshot wounds. Arch Kriminol 1988;181:146–54.
- Pope EJ, Smith OC. Identification of traumatic injury in burned cranial bone: an experimental approach. J Forensic Sci 2004;49:431–40.
- Poppa P, Porta D, Gibelli D, Mazzucchi A, Brandone A, Grandi M, Cattaneo C. Detection of Blunt, Sharp Force and Gunshot Lesions on Burnt Remains: A Cautionary Note. Am J Forensic Med Pathol 2011 [Epub ahead of print]
- Rainio J, Lalu K, Ranta H, Penttila A. Morphology of experimental assault rifle skin wounds. Int J Legal Med 2003;117:19–26.
- Ravreby M. Analysis of long range bullet entrance holes by atomic absorption spectrophotometry and scanning electron microscopy. J Forensic Sci 1982;27:92–112.
- Romolo FS, Margot P. Identification of gunshot residue: a critical review. Forensic Sci Int 2001;119:195–211.
- Ruch RR, Buchanan VP, Guinn VP, Bellanca SC, Pinker RH. Neutron activation analysis in scientific crime detection. J Forensic Sci 1964;9:119–32.
- Rudzitis E, Kopina M, Wahlgren M. Optimization of firearm residue detection by neutron activation analysis. J Forensic Sci 1973;18:93–100.
- Rudzitis E, Wahlgren M. Firearm residue detection by instrumental neutron activation analysis. J Forensic Sci 1975;20:119–24.
- Ruttly GN, Boyce P, Robinson CE, Jeffery AJ, Morgan B. The role of computed tomography in terminal ballistic analysis. Int J Legal Med 2008;122:1–5.

- Sarkis JES, Neto ON, Viebig S, Durrant SF. Measurements of gunshot residues by sector field inductively coupled plasma mass spectrometry—further studies with pistols. *Forensic Sci Int* 2007;172:63–6.
- Schantz B. Aspects on the choice of experimental animals when reproducing missile trauma. *Acta Chir Scand [Suppl]* 1979;489:121–9.
- Schyma C, Placidi P, Schild HH. Radiological findings in gunshot wounds caused by hunting ammunition. An experimental study. *Int J Legal Med* 1996;108:201–5.
- Schwoeble AJ, Exline DL. Current methods in forensic gunshot residue analysis. 2000; CRC Press, Boca Raton.
- Sellier K. Shot Range Determination. *Forensic Science Program Vol. 6*. 1991; Springer, Berlin, Heidelberg, New York.
- Spitz WU, Fisher RS. *Medico-legal investigation of death*. 1973; Charles C. Thomas, Springfield.
- Steffen S, Otto M, Niewoehner L, Barth M, Brozek-Mucha Z, Blegstraaten J. Chemometric classification of gunshot residues based on energy dispersive X-ray microanalysis and inductively coupled plasma analysis with mass-spectrometric detection. *Spectrochim Acta Part B At Spectrosc* 2007;62:1028–36.
- Stein KM, Bahner ML, Merkel J, Ain S. Detection of gunshot residues in routine CTs. *Int J Legal Med* 2000;114:15–8.
- Tschirhart DL, Noguchi TT, Klatt EC. A simple histochemical technique for the identification of gunshot residue. *J Forensic Sci* 1991;36:543–7.
- Tsokos M. Heat-induced post-mortem defect of the skull simulating an exit gunshot wound of the calvarium. *Forensic Sci Med Pathol* 2011;7:227–8.

- Tugcu H, Yorulmaz C, Karslioglu Y, Uner HB, Koc S, Ozdemir C. Image analysis as an adjunct to sodium rhodizonate test in the evaluation of gunshot residues—an experimental study. *Am J Forensic Med Pathol* 2006;27:296–9.
- Türk EE, Anders S, Tsokos M. Planned complex suicide. Report of two autopsy cases of suicidal shot injury and subsequent self-immolation. *Forensic Sci Int* 2004;139:35–8.
- Ubelaker DH. The forensic evaluation of burned skeletal remains: a synthesis. *Forensic Sci Int* 2009;183:1–5.
- Udey RN, Hunter BC, Smith RW. Differentiation of Bullet Type Based on the Analysis of Gunshot Residue Using Inductively Coupled Plasma Mass Spectrometry. *J Forensic Sci* 2011;56:1268–76.
- Ueyama M, Taylor RL, Noguchi TT. SEMS/EDS analysis of muzzle deposits at different target distances. *Scann Electr Microsc* 1980;1:367–74.
- Viel G, Cecchetto G, Fabbri LD, Furlan C, Ferrara SD, Montisci M. Forensic application of ESEM and XRF-EDS techniques to a fatal case of sodium phosphate enema intoxication. *Int J Legal Med* 2009;123:345–50.
- Warlow TA. Firearms, the laws and forensic ballistics. 1996; Routledge, United Kingdom.
- White RS, Owens AD. Automation of gunshot residue detection and analysis by scanning electron microscopy / energy dispersive- X-ray analysis (SEM EDX). *J Forensic Sci* 1987;32:1595–603.
- Wolten GM, Nesbitt RS, Calloway AR, Loper GL, Jones PF. Particle analysis for the detection of gunshot residue. I. Scanning electron microscopy energy dispersive X-ray characterization of hand deposits from firing. *J Forensic Sci* 1979;24:409–22.

LIST OF ARTICLES, ABSTRACTS AND PRIZES

This thesis gave rise to the following articles, congress abstracts and prizes.

Articles published in international peer-reviewed scientific Journals

- Cecchetto G, Giraudo C, Amagliani A, Viel G, Fais P, Cavarzeran F, Feltrin G, Ferrara SD, Montisci M. Estimation of the firing distance through micro-CT analysis of gunshot wounds. *Int J Legal Med.* 2011 Mar;125(2):245-51.
- Cecchetto G, Amagliani A, Giraudo C, Fais P, Cavarzeran F, Montisci M, Feltrin G, Viel G, Ferrara SD. MicroCT detection of gunshot residue in fresh and decomposed firearm wounds. *Int J Legal Med.* 2011 Nov 16. [Epub ahead of print]

Articles published in Italian scientific Journals

- Amagliani A, Fais P, Viel G, Terranova C, Boscolo-Berto R, Giraudo C, Cecchetto G. La TC multi-slice nella determinazione della distanza di sparo. *Zacchia*, 2012, in press.
- Cecchetto G, Giraudo C, Fais P, Nalesso A, Vogliardi S, Amagliani A, Viel G. Determinazione di residui di sparo in ferite d'arma da fuoco putrefatte mediante micro-TC. *Zacchia*, 2012, in press.

Oral communications and poster presented at international and Italian scientific congresses

- Fuzinato DV, Cecchetto G, Fais P, Viel G, Montisci M, Vieira DN. Firearms related deaths in the city of São Paulo, 2006. A retrospective study. XXI International Academy of Legal Medicine Congress, Lisbon, 28-30 May, 2009.
- Viel G, Cecchetto G, Amagliani A, Fais P, Giraudo C, Feltrin GP, Montisci M, Ferrara SD. Micro-CT analysis of gunshot wounds for

- estimating the firing range. 89° Jahrestagung der Deutschen Gesellschaft für Rechtsmedizin, Berlin, 22-25 September, 2010.
- Amagliani A, Fais P, Viel G, Terranova C, Boscolo-Berto R, Giraudo C, Cecchetto G. La TC multi-slice nella determinazione della distanza di sparo. VII Convegno Nazionale Gruppo Italiano Patologia Forense (GIPF), Santa Margherita Ligure, October 21-23, 2010.
 - Cecchetto G, Giraudo C, Fais P, Nalesso A, Vogliardi S, Amagliani A, Viel G. Determinazione di residui di sparo in ferite d'arma da fuoco putrefatte mediante micro-TC. VII Convegno Nazionale Gruppo Italiano Patologia Forense (GIPF), Santa Margherita Ligure, October 21-23, 2010.
 - Cecchetto G, Amagliani A, Viel G, Fais P, Giraudo C, Feltrin G, Ferrara SD, Montisci M. Gunshot wounds covered by different textiles: determination of GSR through micro-CT analysis. 63° Annual Meeting of the American Academy of Forensic Sciences, Chicago, IL, February 21-26, 2011.

Prizes

- 1st Prize in Best Oral Presentation Award at VII Congresso Nazionale del Gruppo Patologi Forensi, Santa Margherita Ligure, October 21-23, 2010.

ACKNOWLEDGEMENTS

This study was conducted in the Laboratory of Forensic Pathology of the Department of Environmental Medicine and Public Health, University of Padova, in collaboration with the Laboratory of Experimental Radiology of the Institute of Radiology – University of Padova.

I am especially grateful to my Tutor, Prof. S. Davide Ferrara, for his support and his precious comments and suggestions that have greatly improved this thesis. He has always had time for my questions and exerted much effort to guide and encourage me through the obstacles during the work.

I want to acknowledge the staff of the Institute of Radiology directed by Prof. Gianpietro Feltrin, especially Dr. Chiara Girauda, for her skillful work in the lab, performing radiological analyses.

I express my warm thanks to my co-authors and friends Dr. Guido Viel, Dr. Paolo Fais, and Dr. Alessandro Amagliani, for their friendly collaboration in all lab work, their help in numerous matters during the last three years and during the preparation of the articles.

I would like to show my gratitude to Dr. Fabiano Cavarzeran and Dr. Rafael Boscolo-Berto for their support to perform the statistical analyses.

I am grateful to Prof. Massimo Montisci, Dr. Gianfranco Fais, and Mr. Ennio Orpini of the Ballistic Laboratory of the “Historical Orpini’s Armoury” for their help in conducting the shooting trials.

Last, but not least, I would like to thank Prof. Franco Tagliaro and the other Professors for the perfect organization of the PhD Course.

Padova, March 14th, 2012

Giovanni Cecchetto